TEMPERATURE PREDICTION MODEL FOR FLOWING DISTRIBUTION IN WELLBORES AND PIPELINES

A

THESIS

Presented to the Graduate faculty

Of the African University of Science and Technology

In Partial Fulfillment of the Requirements

For the Degree of

MASTER OF SCIENCE IN PETROLEUM ENGINEERING

BY

ONUH YUNUSA CHARLES

Abuja-Nigeria

December 2011.

TEMPERATURE PREDICTION MODEL FOR FLOWING DISTRIBUTION IN WELLBORES AND PIPELINES

A THESIS APPROVED BY THE PETROLEUM ENGINEERING DEPARTMENT

RECOMMENDED: …….

Chair, Dr. Alpheus Igbokoyi

…….

Professor Samuel Osisanya

…….

Professor David Ogbe

APPROVED: …….

Chief Academic Officer

……

Date

ACKNOWLEDGEMENT

My gratitude and appreciation to God Almighty who has been faithful in keeping his covenant. In Him, I live, breath and have my being. Without whom I am nothing and indeed, He has promised to do a new thing in my life.

I would like to express my appreciation to my supervisor, Dr. Alpheus Igbokoyi for his encouraging effort in ensuring that this thesis work is a success, thanks for your patience and guidance. I am also grateful to Prof. David Ogbe and Prof Samuel Osisanya for their willingness to serve as members of the thesis committee.

I want to thank my late father, Mr. Onuh Akubor for the countless things he did before passing on to glory, and my sweet mother Mrs. Juliana Akubor for her sacrifice, prayers, and support. To my siblings, Katherine, Victoria, Gloria, Haruna, Paul, Mary, Matthew, Anselem, Job, I thank you all for your support.

I wish to express my indebt gratitude to the lecturers and staff of petroleum engineering department. To Titus Ofei, Azeb Demisi, Omotayo omosebi, oluwabiyi Awotiku, Vita Anye, my brother, Haruna Onuh, my roommate, Joseph Echendu, Destiny Osondu, Mildred Ichiek Ezekiel, and Mr. and Mrs Abu. I couldn't have done much without you guys.

To the petroleum engineering class of 2011, Opeyemi Aborisade, Oscar ogali, Kazeem Adenuga, Nyame Michael, Tony Ikechukwu, and other group members I worked with in several courses, it is a privilege to work with all of you.

TABLE OF CONTENT

LIST OF FIGURES

LIST OF TABLES

ABSTRACT

Down-hole temperature and pressure data are important information needed to understand flowing conditions and production optimization. For example, knowing the wellbore temperature profile is useful in predicting the wax formation in the tubing, which is important in flow assurance.

While gas production usually causes a temperature decrease due to Joule Thomson effect, water entry results in warming of the wellbore. Warmer water entry is as a result of inflow from a warmer aquifer zone due to water coning. Water entry by water coning can therefore easily be detected from temperature profile since it increases the wellbore temperature.

In this study, we successfully developed a temperature prediction model which calculates temperature profiles for flowing temperature in the wellbore and considers Joule Thomson coefficient as a function of mass flow rate of the fluid phases (oil, water, and gas). We modified Alves et al temperature equation and the modified temperature equation was used to produce the work done by Alves et al which produces close result. The model was used to investigate the effect of gas and water entry that created change in temperature profile along the wellbore. The temperature equation can be applied to pipelines or production and injection wells under single phase, two phase, and three phase flow, for horizontal, vertical, and inclined wells.

Cases were considered to verify the effect of water and gas entry into the wellbore. The result shows that water entry increases wellbore temperature and gas entry decreases wellbore temperature and also temperature profile is a function of the flow rate of the fluid. Since the prediction requires the fluid composition in the wellbore, accurate prediction of the temperature profile can give an idea of how much component of each fluid is present in the wellbore.

CHAPTER ONE

GENERAL INTRODUCTION

Down-hole temperature and pressure data are important information to help us understand bottom-hole flow conditions .The temperature and pressure distributions can be measured by production logging or down-hole permanent sensors such as fiber optic distributed temperature sensors (DTS).Correct interpretation of temperature and pressure data can be used to obtain down-hole flow conditions such as oil, gas, and water entry which is used in production optimization. The interpretation of the measured data is often complex due to the multiphase fluid flow in the reservoir. To properly interpret this data, a unified and simplified model is used in predicting the flowing temperature distribution which incorporates the complex process of transient heat transfer between the wellbore and the reservoir.

Distributed temperature sensor technology (DTS) uses a thin glass fiber optical cable installed along the entire well length .Laser light sent through the cable scatters with characteristics that depend on the local temperature. It is then possible to obtain a temperature profile with resolution less than 0.1 ºF, at a distance of several thousand feet, and with a measurement time of typically a few minutes. Unlike a production log that provides only snap shots of the reservoir performance, the DTS enables continuous monitoring of a well to detect temporal changes in the temperature profiles.

1.1 LITERATURE REVIEW

Various investigators proposed approximate analytical solutions for temperature prediction. By making severe assumptions about the pipeline geometry, the heat transfer with the environment, and the

thermodynamic behavior of the flowing fluid, this investigation could obtain explicit expressions for the flowing temperature prediction.

Alves et al [1] (Nov. 1992) presents a general and unified equation for flowing temperature prediction that can be applied to pipelines or production and injection wells under single or two phase flow, over the entire inclination angle range from horizontal to vertical, with compositional and black oil fluid models. The flowing temperature distribution in wellbores and pipelines requires simultaneous solution of continuity, momentum, and energy conservation equations; the solution is further complicated by the thermal interaction between the flow and the environment, especially the reservoir. The derivation of the general and unified equation for temperature prediction applies the conservation laws of mass, momentum, and energy balance. In conclusion, an approximation method for determining two-phase heat capacity and joule Thomson coefficient was proposed and the approximations are useful when generation of enthalpy tables is impossible or inconvenient.

Ramey et al [8] (April 1962) Method usually is used for predicting wellbore temperature distribution, which rigorously incorporates the complex process of transient heat transfer between the wellbore and the reservoir. Ramey's method however is limited to either ideal gas or incompressible liquid flow. It couples heat-transfer mechanism in the wellbore and transient thermal behavior of the reservoir, the transient thermal behavior of the reservoir is determined by solution of the problem of radial heat conduction in an infinite cylinder, the resistances to heat flow In the wellbore, caused by presence of the tubing wall, tubing insulation, fluid in the casing/tubing annulus, casing wall, and cement are incorporated in an overall heat transfer coefficient. Approximate solution to the transient heat conduction problem involved in movement of hot fluids through a wellbore was developed; the approximate solution considers the effect of thermal resistances in the wellbore.

Zhuoyi Li et al [9] (Oct. 2009) present a forward model to predict temperature, pressure, and flow rate of multiphase fluid along a horizontal wellbore. The forward model with inverse model to translate the

observed temperature and pressure data to obtain the oil and water flow rate profile. Stream line simulation method is used to solve the flow problem in the reservoir for fast track of reservoir flow. Transient, three dimensional, multiphase reservoir thermal models is used to calculate reservoir temperature. The reservoir flow model and thermal model with a horizontal well temperature model is used to predict the pressure and temperature distribution in a horizontal well system. The inversion method, that is, the traditional Markov chain Monte Carlo Method (MCMC) is used to interpret the pressure and temperature data to obtain flow rate profile along horizontal well. The result shows that 3D transient flow simulation of reservoir flow and temperature is more flexible than the previously developed 1D model. The simulation flow field as a function of producing time improves understanding of down-hole flow condition. Secondly, the transient flow effect on temperature behavior can provide additional information on the location of water entry.

Yoshioka et al [10] (Nov. 2007) presents a paper that interprets distributed temperature and pressure data to obtain flow rate profiles along horizontal well, it incorporates an inversion method that is based on Levenberg-Marquardt algorithm , applied to minimize the differences between the measured profiles and profile calculated from a forward model of the well and reservoir flow system. The research proposes an inversion method to obtain down-hole flow conditions from temperature and pressure profile data, the inversion method based on Levenberg-Marquardt algorithm inverts the continuous temperature and pressure data along the well obtained by the forward model. Synthetic and field examples are also presented to illustrate how to use the inversion model to interpret the flow profile of a horizontal well. In the Result, synthetic examples showed that even with single-phase oil production, the inflow profile may be estimated. The method is more robust when water or gas is produced along discrete intervals in oil producing well because of the unique temperature signature of water or gas production. They applied inversion method to temperature and pressure profiles measured with production logs in North Sea horizontal oil and water producing well, the inversion

method successfully matched the profile of temperature and pressure to determine the inflow profiles of oil and water.

Ochi et al [11] (Oct. 2008) developed a model to predict well flowing temperature and pressure (i.e. the forward model), and applied an inversion method to detect water or gas entry into the wellbore using synthetic data generated by the forward model (i.e. an inversion model). It is concluded that temperature profiles could provide sufficient information to identify fluid entries, especially in gas wells. The study focuses on the field application of the developed mode. The predicted temperature and pressure profiles from the forward model were used to history match field data while the inversion process inferred the inflow profile of gas and water along the wellbore checking against the interpretation of production logging. The interpretation model for down-hole flow conditions from the temperature and pressure data is a coupled wellbore/reservoir flow model. The model is built on flow and energy conservation equation for both the reservoir and wellbore. These equations are mass balance equation, Darcy's law, and energy (momentum) balance equation. The interpretation model assumes steady state flow condition in the reservoir, one-dimensional (1-D) inflow from the reservoir, isolated reservoir segments, single phase flow in a reservoir segment (segregated reservoir flow). From the study, it was shown that for single phase oil producing well, the interpretation model can estimate inflow distribution if the measurement of temperature and pressure along the wellbore is available. Secondly, when a gas well produces water from the bottom zone, higher entry temperature of fluid than geothermal temperature suggests water coning. Thirdly, other than bottom perforation, gas inflow causes temperature decrease, and water entry slows down temperature decline at water entry locations. Pressure data has less indication of water entry if water does not enter from the bottom. Fourthly, water detection may depend on water to gas volume ratio. For this study, when water/gas ratio is greater than 0.03 bbl/Mscf, the interpretation model gives reasonable results.

Octavio et al [12] (Dec. 2005) proposed a one-dimensional, time dependent homogeneous mathematical model which can be used to determine pressure, temperature, and velocity distributions of two-phase flow with (water-oil and gas) in oil wells. The numerical solution of the mathematical model, which consist of mass, momentum, and energy conservation equations, is based on the finite difference technique in the implicit scheme. The thermodynamic and transport properties of the fluid are estimated by black oil PVT correlations.

Jacques et al [13] (Dec. 2004) presented a work that to assess Ramey's classic method for the calculation of temperature in injection and production wells, it showed that Ramey's method is an excellent approximation except for an early transient period in which the calculated temperatures are significantly overestimated, a simple graphical correlation to estimate the length of this early transient period. They further demonstrated that Ramey's procedure for the estimation of overall heat transfer coefficients holds good only for Fourier dimensionless time. The dimensionless time in the Fourier equation is determined by the thermal diffusivity of the formation and thus is different from the dimensionless time in the tubing heat balance. The inspection analysis of the Ramey wellbore heat transmission equations shows that temperature distribution in a wellbore is governed by three dimensionless numbers: Graetz number, Ramey number, and thermal skin factor.

Yoshioka et al [14] (April 2006) illustrated range of inflow conditions for which water or gas entry locations can be identified from the temperature profile of a well from measurable temperature changes. Two different models were used in this study. For water coning, a 3-D reservoir model is used, the top and side of the reservoir were sealed, and the pressure below the reservoir (aquifer pressure) is constant. For water produced from the same elevations as the oil, a 1-D reservoir model was used. Warmer water entry, cooler water entry, and cooler gas entry was analyzed from the generated temperature and pressure profiles for two- phase oil- water flow or two-phase oil- gas flow in the horizontal well. In summary, if water production is caused by water coning from a deeper formation, it will cause a

wellbore temperature increase. If water comes from the formation at the same elevation, water production often causes a wellbore temperature decrease. Secondly, gas production causes a temperature decrease. Gas production at the toe is detectable even if the total production rate is small. When gas enters at the middle of the wellbore, its temperature change can be observed for higher gas production rates. Thirdly, the temperature difference caused by water entry is sensitive to the producing zone and for the case that water entry zone is short, it is very hard to locate the water entry.

Hani et al [15] (Oct. 1999) showed that temperature records in gas well tests can also be used to explain anomalous pressure trend and assess the quality of the test data and test procedures, the objective of this work has been to provide a better understanding of temperature behavior in gas well test by reviewing the various wellbore temperature models available and by presenting simplified models that could be used to utilize the temperature data in well tests. In conclusion, it was shown that a general model of temperature behavior during well tests needs to couple an overall energy balance with a number of transport laws. Secondly, temperature records can be very useful for quality control and verification of the pressure data recorded during drawdown tests. Thirdly, it was also shown that if gauges are close enough to the perforation, the temperature behavior in the wellbore is dominated by Joule Thomson heating/cooling during flow. Fourthly, if gauges are far enough from the perforations, the temperature behavior in the wellbore is heavily affected by unsteady state conduction. This effect is largely proportional to flow rate.

1.2 PROBLEM STATEMENT

There are many previous attempts in developing model for temperature profile for two phase mixture in wellbore and pipelines in inclined wells, vertical wells and horizontal wells. In the oil and gas industry today, the advancement of down-hole data in wells requires interpretation and application of the data

in improving production performance and reducing cost. Fluid production in the wellbore usually occur in three phase of oil, water, and gas, which affect the flowing temperature distribution.

This research work is aimed at modeling flowing temperature distribution for three phase, identifying fluid type and properly analyzing the effect of fluid type on temperature profile in the wellbore.

1.3 OBJECTIVES

This study presents a general and unified equation for flowing temperature prediction which can be applied to pipelines or production and injection wells, under single phase, two-phase and three-phase flow over the inclination angle range from horizontal to vertical with compositional or black oil fluid models. The temperature prediction model is used to demonstrate the size of temperature change and to investigate how the origin, amount, and types of fluid entering a well affect temperature profiles. It requires simultaneous solution of continuity, momentum, and energy conservation equations. The solution is further complicated by the thermal interaction between the flow and the environment, especially the reservoir. [1]

a. Study the application of temperature measurement from distributed temperature sensing.
b. To develop a analytical model that predicts wellbore temperature fluid for three phases.
c. To demonstrate the size of temperature changes caused by the flow rates and to investigate how the origin, amount, and types of fluid entering a well affect temperature profiles.
d. Explain the meaning and variations in temperature profiles and their value for monitoring well performance.

1.4 THESIS ORGANISATION

This thesis is organized into six chapters. The first chapter presents the introduction, literature review, problem statement, and objectives. The second chapter provides theoretical background of the subject.

Section 2.1 provides basic concept and terminology of temperature logs. Section 2.2 provides basic concept and application of distributed temperature sensing. Section 2.3 provides interpretation and analysis of temperature log in horizontal well. Section 2.4 provides detail information on the effect of classic liquid and gas entries. Chapter three discusses the development of the simplified temperature equation for flowing temperature prediction, it can be applied to pipelines or production and injection wells, under single phase, two-phase, and three-phase, over the entire inclination angle range from horizontal to vertical, with compositional and black oil models. Chapter four provides a step by step procedure for the programming using Matlab. Chapter five discusses the result obtained from the application of the model. Chapter five gives conclusion and recommendation from the study.

CHAPTER TWO

REVIEW OF TEMPERATURE LOGS

2.1 TEMPERATURE LOGS

Continuous temperature logs are used to digitally record wellbore temperature versus depth. Comparison of temperature anomalies to the normal geothermal gradient provides valuable information about the location and nature of fluid movement around the tool and behind the pipe.

2.1.1 HEAT BALANCE

As fluid moves through the pipe, it continuously gains or losses heat to the ground by conduction. The temperature profile in the fluid is affected by *elevation changes, velocity changes, heat transfer and joule Thomson heating or cooling effects*.[5]

The heat transfer to the surroundings, *q*, is a function of the average fluid temperature in the increment and the corresponding ground temperature. It can be determined by the use of the concept of the overall heat-transfer coefficient, *U.* [5]

$$q = U(T - Te) \quad (2.1)$$

The overall heat transfer coefficient is a combination of three terms:

a. Heat conduction through the surrounding soil, hs
b. Heat conduction through the pipe wall and insulation, hp and
c. Convective transfer from the pipe wall to the fluid. hf

The overall heat transfer coefficient is given by, [5]

$$\frac{1}{U} = \frac{1}{h_s} + \frac{1}{h_P} + \frac{1}{h_f} \quad (2.2)$$

2.1.2 WELLBORE HEAT TRANSFER

When hot reservoir fluids enter a wellbore and begin to flow to the surface, they immediately begin to lose heat to the cooler surrounding rock. The surrounding rock gradually heats up, reducing the temperature difference and heat transfer between the fluids ant the rock. Eventually, for a constant mass flow rate, the earth surrounding the well reaches a steady-state temperature prediction. Prediction of fluid temperatures in the wellbore as a function of depth and time is necessary to determine the fluid's physical properties and calculate pressure gradient.

Heat transfer within the tubing and in a fluid-filled annulus is primarily am result of convection. Heat transfer through the tubing and casing walls and through a cement-filled annulus between the casing and borehole wall primarily result from conduction.

2.1.3 GEOTHERMAL TEMPERATURE

The temperature that naturally increases with depth is known as geothermal temperature, it is observed that temperature increases with depth since heat is transferred from inside the earth to its surface, the rate of increase depends on the types of rock layers and their thermal conductivity. Fourier's law of heat conduction states that the heat flux by conduction is proportional to the temperature gradient.

Mathematically,

$$\bar{e}_{cond} = -K_{Tt} \nabla T \qquad (2.3)$$

Where,

K_{Tt}= total thermal conductivity including rock and fluid, in the rock layers which is treated as a constant over particular rock layers, although it is actually a function of the constituent minerals and fluid within the rocks .

$\bar{e}_{cond}$= heat flux (rate of thermal energy transfer per unit area) which is approximately constant with depth .

∇T = temperature gradient, the minus sign (-) shows that the transfer in the direction of decreasing temperature

The slope of the geothermal temperature profile in each rock layers depends on it's thermal conductivity, The higher the thermal conductivity of a rock layer, the lower the slope across it.

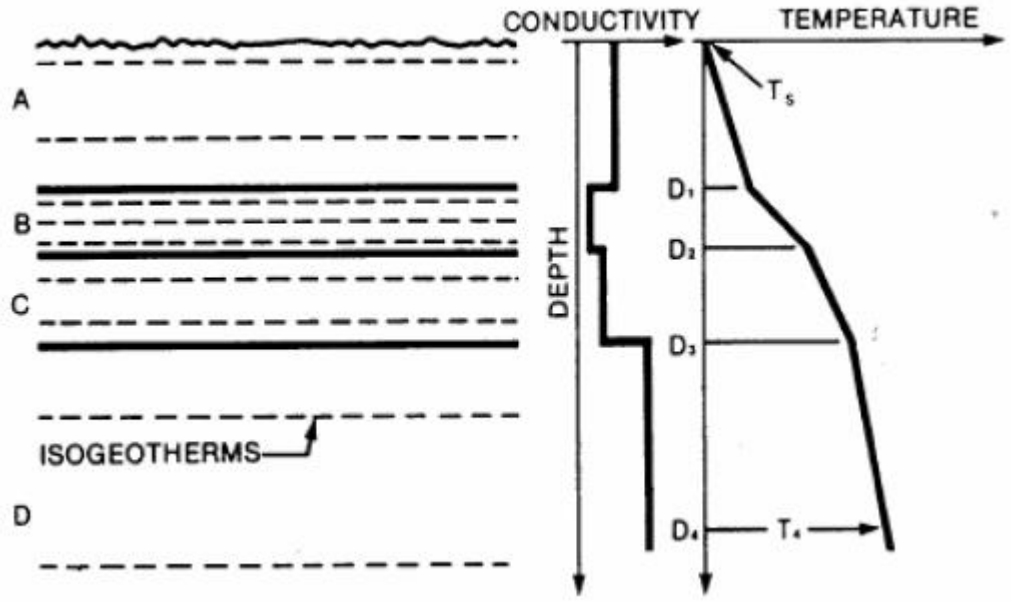

Fig.2.1 Sketch of geothermal temperature profiles (right) for different formations. [From Jorden and Campbell (1984)].

2.1.4 JOULE THOMSON EFFECT

Joule's law of heating states that the amount of heat produced each second in a conductor by a current of electricity is proportional to the resistance of the conductor and square of the current.

Enthalpy is a direct function of temperature and pressure. When pressure drops through a valve, we normally expect temperature to rise for liquid dominated flow and to drop for vapor dominated flow. Temperature change resulting from expansion is referred to as a *Joule- Thomson effect.*

The temperature behavior of a fluid during a throttling (h = constant) process is described by the *Joule Thomson coefficient*.

Joule Thomson coefficient is a measure of the change in temperature with pressure during a constant enthalpy process.

$$\eta = \left[\frac{\partial T}{\partial P}\right]_h \tag{2.4}$$

During a throttling process [7],

$$\eta = \begin{cases} < 0 \ temperature\ increases \\ = 0 \text{ temperature remains constant} \\ > 0 \ temperature\ decreases \end{cases}$$

A throttling process proceeds along a constant enthalpy line in the direction of decreasing pressure, that is, from right to left. Therefore, the temperature of the fluid increases during the throttling process that takes place on the right hand side of the inversion line. The frictional cooling noticed in gas pipelines is also a Joule-Thomson effect. When heat loss, potential, and kinetic energy are negligible, the gas temperature will drop solely because of pressure drop (friction) at constant enthalpy. This effect can cause the gas temperature to drop below ground temperature.

The temperature of the fluid changes when a fluid expands at constant enthalpy, this is referred to as Isenthalpic process because of pressure drop). This phenomenon is called *Joule –Thomson effect,* the temperature change per unit pressure change is called *Joule-Thomson coefficient*, η

Maxwell relation of thermodynamics is,

$$dU = Tds - PdV \qquad \rightarrow \left[\frac{\partial s}{\partial P}\right]_T = -\left[\frac{\partial V}{\partial T}\right]_P \tag{2.5}$$

$$dh = Tds + VdV \quad \rightarrow \left[\frac{\partial s}{\partial V}\right]_P = \left[\frac{\partial P}{\partial T}\right]_s \tag{2.6}$$

$$da = -sdT - PdV \quad \rightarrow \left[\frac{\partial P}{\partial T}\right]_V = \left[\frac{\partial s}{\partial V}\right]_T \tag{2.7}$$

$$dg = -sdT + VdP \quad \rightarrow \left[\frac{\partial V}{\partial T}\right]_P = -\left[\frac{\partial s}{\partial P}\right]_T \tag{2.8}$$

For constant enthalpy,

$$\Delta h = 0 \tag{2.9}$$

For pure fluid, the fluid enthalpy is a function of temperature and pressure, expanding the above equation in the following way

$$\left[\frac{\partial h}{\partial T}\right]_P \Delta T + \left[\frac{\partial h}{\partial \rho}\right]_T \Delta P = 0 \tag{2.10}$$

Applying definition of heat capacity and Maxwell's relation of thermodynamics

$$C_P \Delta T + \left[V - T\left[\frac{\partial V}{\partial T}\right]_P\right] \Delta P = 0 \tag{2.11}$$

Specific volume, $V = \frac{1}{\rho}$, (2.12)

$$\left[\frac{\partial V}{\partial T}\right]_P = \left[\frac{\partial (\frac{1}{\rho})}{\partial T}\right]_P = \frac{-1}{\rho * \rho}\frac{\partial \rho}{\partial T} \tag{2.13}$$

Replacing the specific volume with the fluid density

$$C_P \Delta T + \left[\frac{1}{\rho} - \frac{T}{\rho}\left(-\frac{1}{\rho}\right)\left[\frac{\partial \rho}{\partial T}\right]_P\right] \Delta P = 0 \tag{2.14}$$

Substituting the definition of thermal coefficient, $\beta = \left(-\frac{1}{\rho}\right)\left[\frac{\partial \rho}{\partial T}\right]_P$ into the above equation

$$C_P \Delta T + \left[\frac{1}{\rho} - \frac{\beta T}{\rho}\right] \Delta P = 0 \tag{2.15}$$

Rearranging the above equation gives expression for η

$$\eta = \left[\frac{\partial T}{\partial P}\right]_h = \frac{\beta T - 1}{\rho C_P} \tag{2.16}$$

For an ideal gas, $\beta = 1/T$and Joule Thomson coefficient is zero, which means that when an ideal gas expands as the enthalpy is constant, there is no temperature change. As real fluids expand, cooling occurs if η is positive, while warming occurs if it is negative.

Fluid flow in a reservoir can be approximated as an isenthalpic flow neither heat nor work done on the fluid). During production, the Joule Thomson effect is a dominant factor causing the inflow temperature of the fluid to be different from the geothermal temperature at that depth.

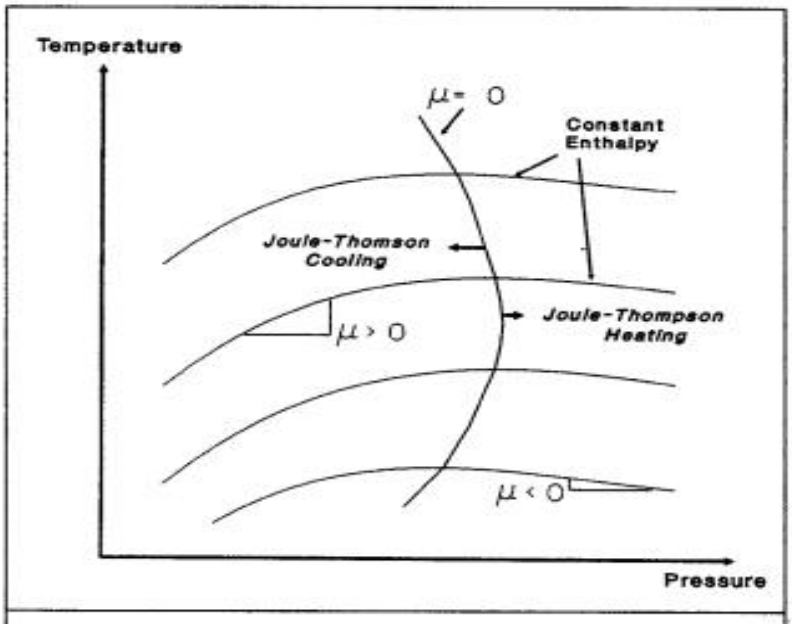

Fig.2.2 Enthalpy curves for a typical hydrocarbon mixture illustrating the Joule Thomson effect [From Rajiv et al (1991)]

The Joule Thomson coefficient determines the amount of cooling or heating caused by pressure changes within a fluid flowing up the well. Using thermodynamic principles, the Joule Thomson coefficient is determined from an equation of state for Particular fluid mixture.[19]

$$\eta = \left[\frac{\partial T}{\partial P}\right]_h = \frac{1}{C_p}\left[T\left(\frac{\partial T}{\partial V}\right)_p - V\right] \qquad (2.17)$$

Temperatures and pressures where the slope of the constant-enthalpy curve is positive correspond to Joule Thomson cooling. Conversely, when the slope is negative, joule Thomson heating occurs. Joule

Thomson cooling is much more significant than Joule Thomson heating for typical range of temperatures, pressures, and two phase fluid mixtures encountered in a flowing well. Joule Thomson heating typically occurs in some gas condensate systems and could be determined from mixture composition. Joule Thomson cooling is usually associated with a high gas component in two phase mixture. Hence wells having relatively high liquid holdups caused by either low gas/liquid ratios or higher wellhead pressures, will experience little joule Thomson heating or cooling. However for wells operating with low liquid holdups, joule Thomson cooling could be more significant.

2.2 DISTRIBUTED TEMPERATURE SENSING

DTS stands for Distributed Temperature Sensing.DTS is a technology which provides the user with a technique to measure the temperature distribution along a fiber optic line at any time and to repeat such measurements as required, the fiber-optic technology has made down-hole temperature measurement very accurate and reliable. The fiber optic line can be any length up to about 30km (about 18.5 miles). With the exception of the recording instrumentation at one or both ends of the fiber, there are no electronics, no sensors, no electrical wires or electrical connections along the line. The line may be permanent or reinstalled for each use. It is inherently safe to use in environments where an electrical spark may pose a fire safety hazard.[2]

2.2.1 APPLICATION OF DISTRIBUTED TEMPERATURE SENSING

A DTS has applications wherever the temperature distribution is useful. For example, a fiber optic DTS line may be tied to an electrical power line.[2] DTS is most often used where temperature changes in time indicate the onset of deviant behavior or imminent failure of some system. Oil wells can be monitored periodically to detect the onset and location of anomalous fluid production, one obvious use for DTS surveys is well monitoring on a pad or production platform. Weekly monitoring can detect changes in

the well temperature profile. When such changes occur, the well's production can be tested to determine the cause of the temperature change. Immediate action can be taken to remedy or shut-in the non-performing well .[2]

TOOL APPLICATIONS

a. Locate liquid or gas entry points
b. Detect leaks
c. Detect channels behind pipe
d. Locating lost circulation zones
e. Determining bottom-hole temperature (assumed to be the maximum temperature)

2.2.1.1 LOCATE TOP OF CEMENT

The temperature log detects top of cement by realizing that the curing of cement consist of exothermic reactions, the two main reactions that release energy when water is added to cement, which is mainly composed of tricalcium silicate and dicalcium silicate.

$2Ca_3SiO_5 + 7H_2O \rightarrow 3CaO.2SiO_2.4H_2O + 3Ca(OH)_2 + 173.6KJ$

$2Ca_2SiO_4 + 5H_2O \rightarrow 3CaO.2SiO_2.4H_2O + Ca(OH)_2 + 58.6KJ$

A large amount of thermal energy (232.2KJ from both reactions per two moles of both silicates) cause a rise of wellbore temperature that can be easily be detected with a temperature log.

2.2.1.2 DETECT CASING LEAKS AND CHANNELS

Temperature logs combined with production logs such as spinner flowmeter can give a unique interpretation; a deviation of wellbore temperature profile from the geothermal temperature profile indicates there is an upward flow of fluid entry from bottom zone.

2.2.1.3 ESTIMATE FLOW RATE

In production well, fluid enters the wellbore at the geothermal temperature if Joule- Thomson effect is neglected. While the fluid flows up the well, it conductively loses thermal energy to the casing and the surrounding formation. As a result the temperature profile of the flowing fluid is concave upwards towards the geothermal temperature profile. At higher depth, the temperature curve becomes parallel to the geothermal temperature profile. As shown in the figure below, the separation between the asymptotic portion of the temperature log and the geothermal temperature profile is mainly a function of the flow rate.

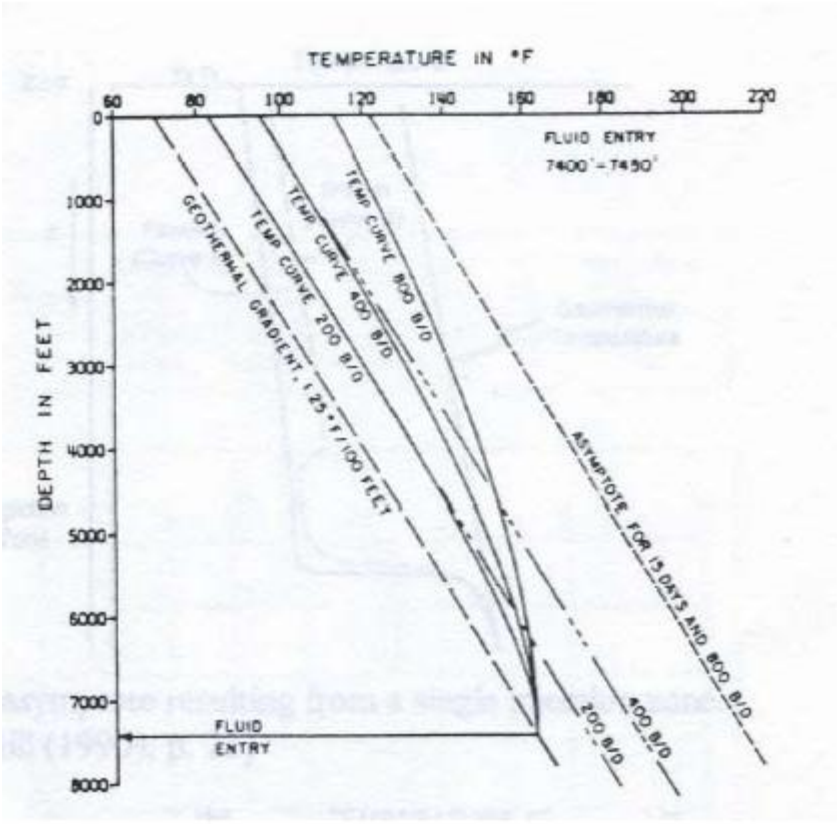

Fig.2.3 Application of temperature log to estimate flow rate [FROM CURTIS AND WITTERHOLT (1973)]

2.3 INTERPRETATION OF TEMPERATURE LOGS IN PRODUCING WELLS

This section reviews and provides the basics of temperature log interpretation and what happens to a fluid's temperature as it enters and flows along the borehole, assuming that the temperature survey is taken within the fluid flow, as would be the case if a logging tool is run in the well. This implies that DTS survey is usually taken either in the annulus or in the cement sheath. Therefore, the temperature measured by a distributed temperature sensing is not the flowing fluid temperature, but some value between the flowing borehole fluid and the formation. [2]

2.3.1 TEMPERATURE ANALYSIS IN HORIZONTAL WELL

Analyzing temperature profiles in horizontal well is usually challenging due to the following:

a. The flow geometry of horizontal well is much more complex than vertical wells because the flow is constrained by the horizontal reservoir boundaries, certain assumptions has to be made to derive both the flow and temperature models.
b. Geothermal temperatures along a horizontal well are almost constant
c. The size of the temperature is usually small, so it is crucial to include subtle thermal energy effect, heat convection, fluid expansion, viscous dissipation, and thermal conduction.

2.4 Temperature interpretation

Temperature logs have been used successfully in vertical wells to locate gas entries, detect casing leaks, evaluate cement placement, and estimate inflow profiles. Temperature interpretation are now used In identifying types of fluid flowing to a wellbore , and intelligent well technology can be used to isolate the unwanted fluid.

2.4.1 CLASSIC LIQUID ENTRIES

The effects of liquid flow on a temperature log are illustrated on Fig. 2.4. As the earth is penetrated to deeper depths, the temperature increases. This rate of temperature increase, called the "*Geothermal Gradient*" or "*Geothermal Profile*" and this may vary, depending on the adjacent formation or depth, differences in thermal conductivities of rocks between the bottom of the hole and the surface, and fluctuations in the surface temperature which penetrates the sub-surface and perturb the sub-surface temperature, low thermal conductivity rocks, such as shale, act as thermal insulator and have a large temperature gradient across them, while high thermal conductivity rocks, such as salt, permit the conduction of heat efficiently, and have a small temperature gradient across them. However, it is generally assumed that the geothermal gradient is constant over the logged interval, and the effects of liquid movement cause some deviation from the geotherm. Geothermal gradients vary from about 0 .5 to 2.0 degF/100ft or 0.9 to 2.7 degC/100m.[2]

In Fig. 2.4, the borehole below B is static, and referred to as a "static rat hole". However, there is a liquid flow (no solution gas) in a channel behind pipe from A to A'. The liquid enters the channel at the temperature of the geothermal gradient, i.e., its formation temperature. As the liquid moves from "A" downward, it is moving into a channel which grows hotter with depth, and as a result the liquid heats up a bit before exiting into a formation at A'. Since the borehole fluid in this interval is static, it soon takes on the temperature of the nearby channel. Both above A and below A', the rathole temperature is that of the geothermal gradient. Note that if flow entered the wellbore and flowed from A to A' the temperature log would look qualitatively the same.[2]

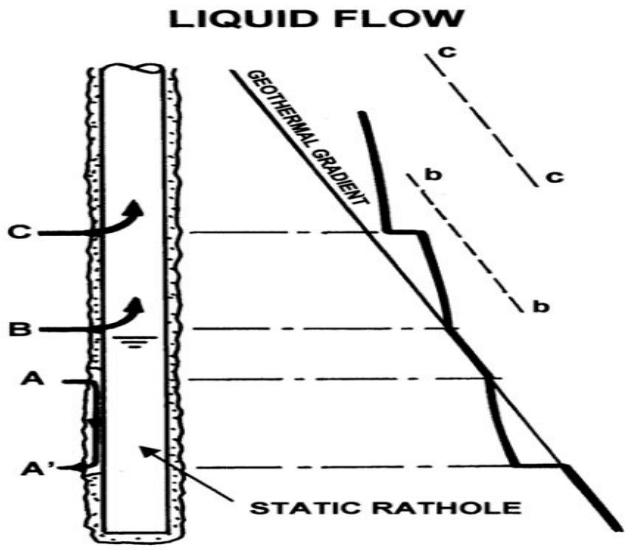

FIG.2.4 Schematic showing liquid crossflow, a to a ', and entries at B and C [From James (2003)]

The first entry into the wellbore occurs at B. The liquid enters at its formation temperature and moves uphole. It is flowing into a borehole which is cooler. As a result, the liquid temperature is greater than the geothermal and cooling as it moves uphole. When another entry occurs, as at C, the effect is to mix the two flows, thereby causing a cooling effect on the log at C, The relative position of the resultant mixture between the geotherm and the upcoming flow from B may be a quantitative indication of the relative proportions of the two flows in the new mixture above C. Any quantitative evaluation would require that the fluids from below and entering at C have the same heat capacity.[2]

Note the dashed lines bb and cc in the figure. If the wellbore didn't change and the flow from B could continue uphole, it would asymptotically approach a straight line parallel to the geothermal profile. The displacement of bb from the geotherm would be greater with increasing flow rates. Note that the resultant flow from mixing B and C would approach an asymptote further to the right, indicated by the line cc.[2]

There may be some exceptions to the above guidelines. A liquid entry may cause a heating anomaly at the point of entry. This often occurs when a water entry is the first entry from the well bottom. This

effect is called a *Joule-Thompson heating* and can be as much as 3 ºF per 1000 psi pressure drawdown from the formation. This is often referred to as *friction heating*. It is less likely at oil entries since a large drawdown may cause solution gas to be released and result in a cooling anomaly at the point of entry.[2]

2.4.2 CLASSIC GAS ENTRIES

The Effects of a gas flow are shown on Fig. 2.The flow profile is much like the previous section. There is a down-moving channel from A to A'. The entry of gas into the channel causes a cooling effect due to the *adiabatic expansion of the gas*. This cooling effect is detected in the "static rathole" as is the temperature along the channel.[2]

The entry at B causes a cooling effect. When the gas moves uphole, it is moving into a hotter environment and begins to heat up. The entry at C causes another cooling effect as shown. Strictly speaking, the entry at C need only be cooler than the geothermal and so may cause a slight heating of the fluid moving up from B. In any case this resultant flow crosses the geothermal where it is cooled by a new entry at D. Note that the entry at D must be a cooling anomaly. Once above the geothermal gradient, every entry (with the possible exception of the Joule-Thompson heating effect mentioned above) must be a cooling anomaly on the log.[2]

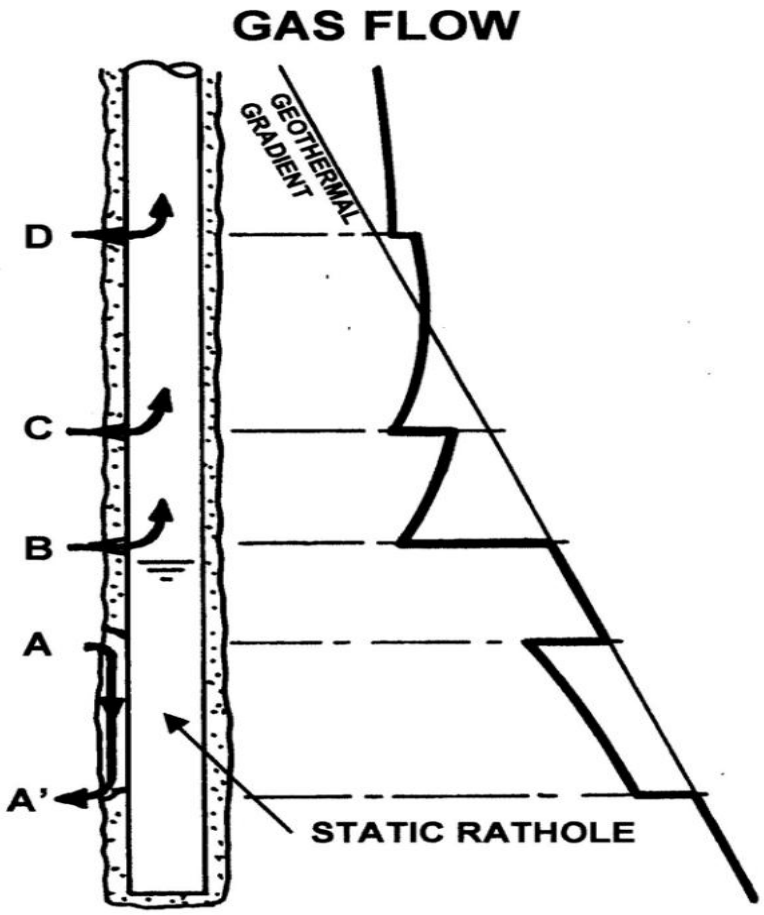

fig.2.5 Schematic showing gas crossflow (A to A') and gas entries at B, C, and D. [From James (2003)]

Gas entry zone can be identified from a wellbore temperature profile from the knowledge of Joule Thomson effect. As can be seen from the diagram below, the inflow temperature of the gas from the middle zone is cooler than the geothermal temperature. Also, the mixing between the inflow gas and the wellbore flow lowers the mixed temperature below the geothermal temperature, the middle zone is obviously the gas zone based on the large cooling anomaly on the temperature profile. However all cooling anomalies are not gas entry, the liquid that enters the wellbore at the shallower depth can cause cooling anomaly. Here the oil tends to enter the wellbore at or slightly above the geothermal temperature. The entry oil mixes with the warmer flow from below, and as a result, the new mixed flow

is at a temperature between the two (i.e. between the warmer flow from below and the entry oil mixing with the inflow as is flows upward).

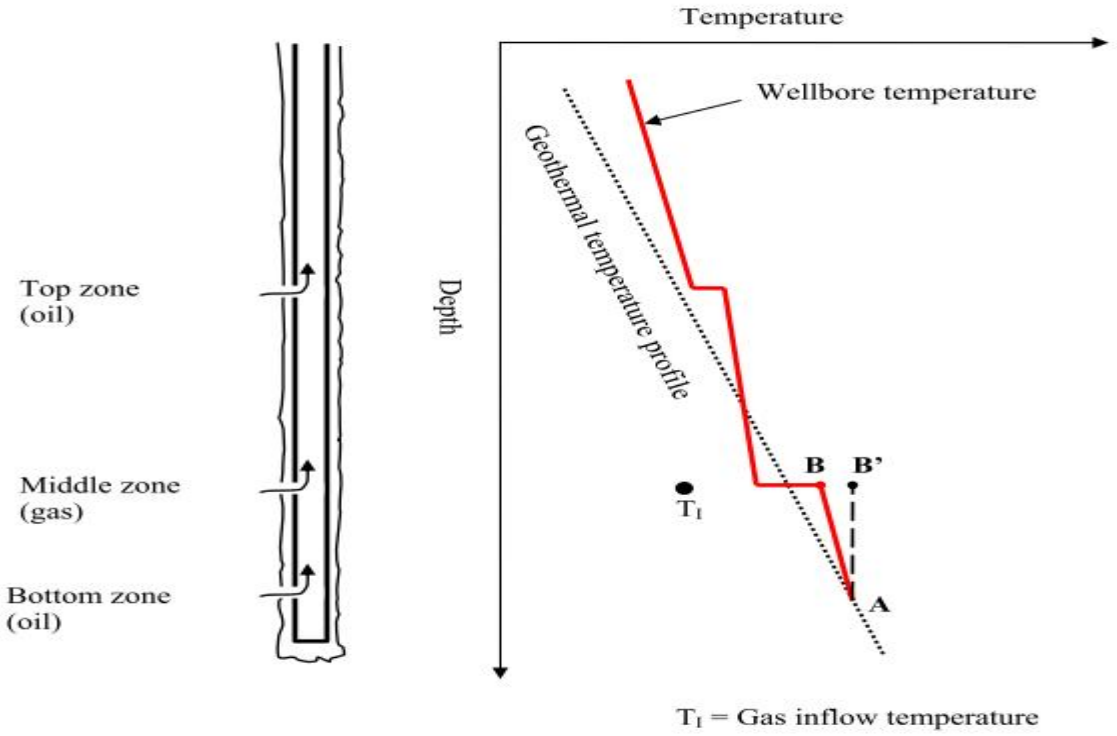

Fig.2.6 Detection of gas entry on a temperature profile by the Joule Thomson effect [From Pinan (2006)]

CHAPTER THREE

ANALYTICAL TEMPERATURE MODEL

3.1 MODEL DEVELOPMENT

For a vertical well, it is reasonable to assume that the pressure drop caused by friction along the well is negligible. This is mainly because the length of the well that is in contact with the reservoir is short and an inconsiderable pressure drop is expected in such short wellbore within the practical ranges of vertical well production rates. For a horizontal well, neglecting the influence of long wellbore pressure drop could lead to an error in estimating the inflow rate distribution along the wellbore.

3.2 MODEL GEOMETRY

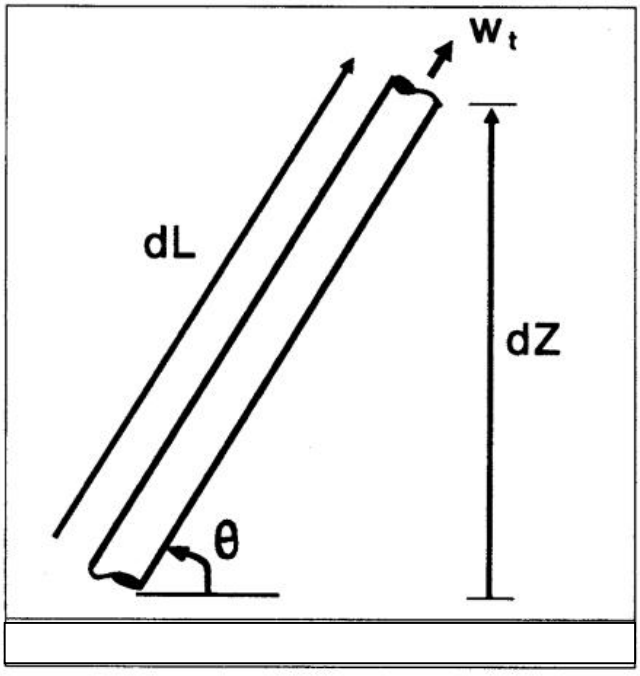

Fig.3.1 sign convention for flowing well . [From Rajiv et al (1991)]

3.3 DERIVATION OF GOVERNING EQUATION

The derivation of the general and unified equation for temperature prediction involves the conservation laws of mass, momentum, and energy balance to a differential control volume of a pipeline.

The basis for virtually all computations involving fluid flow in pipes is conservation of mass, momentum and energy equation. Application of these principles enables calculation of changes in pressure and temperature with distance.

ASSUMPTIONS

The assumption below is same as that of Alves

1. Surrounding temperature is a linear function of depth
2. Steady state flow process (pressure change with time is zero)
3. Temperature of fluid at pipe intake is equal to environmental temperature at pipe intake.

3.3.1 CONSERVATION OF MASS PRINCIPLE

The law of conservation of mass' states that mass cannot be created or destroyed. The conservation of mass principle for a control volume can be expressed as: *the net mass transfer to or from a control volume during a time interval Δt is equal to the net change (increase or decrease) in the total mass within the control volume during Δt .*That is

$$\left(\begin{matrix}\text{TOTAL MASS ENTERING THE}\\ \text{CONTROL VOLUME DURING } \Delta t\end{matrix}\right) - \left(\begin{matrix}\text{TOTAL MASS LEAVING THE}\\ \text{CONTROL VOLUME DURING } \Delta t\end{matrix}\right) =$$

$$\left(\begin{matrix}\text{NET CHANGE IN MASS WITHIN}\\ \text{THE CONTROL VOLUME DURING } \Delta t\end{matrix}\right) M_{in} - M_{out} = \Delta M_{cv} \qquad (3.1)$$

Where $\Delta M_{CV} = M_{final} - M_{initial}$ is the change in the mass of control volume during the process.

Considering a control volume of arbitrary shape, the mass of differential volume $\boldsymbol{dV}$within the control volume is $\boldsymbol{d}M = \boldsymbol{\rho\ dV}$

The total mass within the control volume at any instant in time t is determined by integration to be:

Total mass within the control volume,

$$M_{CV} = \int_{CV} \rho dV \quad (3.2)$$

Then the time rate of change of the amount of mass within the control volume can be expressed as:

Rate of change of mass within the control volume, $\frac{dm_{cv}}{dt} = \frac{d}{dt}\int_{CV} \rho dV$ (3.3)

For special case of no mass crossing the control surface (i.e., the control volume resembles a closed system) the conservation of mass principle reduces to that of a system that can be expressed as $dM_{CV}/dt = 0$.This relationship is valid whether the control volume is fixed, moving, or deforming.[7]

3.3.2 MOMENTUM CONSERVATION PRINCIPLE

The law of conservation of momentum states that for a collision occurring between two objects in an isolated system, the total momentum of the two objects before collision is equal to the total momentum of the two objects after collision.

3.3.3 ENERGY CONSERVATION EQUATION

The first law of thermodynamics, also known as the conservation of energy principle states that energy can neither be created nor destroyed during a process, it can only change forms.

In the light of the preceding discussion, *the conservation of energy principle can be expressed as* the net change (increase or decrease) in the total energy of a system during a process is equal to the difference

between the total energy entering and the total energy leaving the system during that process. $\left(\begin{smallmatrix}\text{TOTAL ENERGY}\\ \text{ENTERING THE SYSTEM}\end{smallmatrix}\right) - \left(\begin{smallmatrix}\text{TOTAL ENERGY}\\ \text{LEAVING THE SYSTEM}\end{smallmatrix}\right) = \left(\begin{smallmatrix}\text{CHANGE INTHE TOTAL}\\ \text{ENERGY OF THE SYSTEM}\end{smallmatrix}\right)$

$$E_{in} - E_{out} = \Delta E_{system}$$

Applying steady-state mass, momentum, and energy balance to the differential control volume.

The conservation of mass simply means that for a given control volume, such as a segment of pipe, MASS IN minus the MASS OUT must equal the MASS ACCUMULATION). For a constant area duct,

$$\frac{\partial P}{\partial T} + \frac{\partial(\rho v)}{\partial L} = 0 \qquad (3.4)$$

For steady state flow, no mass accumulation can occur, then equation above becomes

$$\frac{d}{dL}(\rho V) = 0 \quad \text{(Mass balance equation)} \qquad (3.5)$$

Using equation (1), it is evident that steady state flow is characterized by $\rho v = constant$

Applying Newton's first law to fluid flow in pipes requires that the rate of momentum out, minus the rate of momentum in, plus the rate of momentum accumulation in a given pipe segment must equal the sum of all forces on the fluids. *The conservation of linear momentum* can be expressed as, [15]

$$\frac{d}{dL}(\rho V^2) = -\frac{dP}{dL} - \rho g \sin\theta - \frac{\tau \pi d}{A_P} \text{ (Momentum balance equation)} \qquad (3.6)$$

Applying energy conservation to fluid flow in pipes requires that in a given pipe segment, the energy in, minus the energy out, plus the heat energy to or from the surroundings must equal the rate of energy accumulation. [15]

$$\frac{d}{dL}\left[\rho V\left(e + \frac{1}{2}V^2\right)\right] = -\frac{d}{dL}(PV) - \rho V g \sin\theta - \frac{q \pi d}{A_P} \quad \text{(Energy balance equation)} \qquad (3.7)$$

From equation (2)

$$\frac{dP}{dL} = -\frac{d}{dL}(\rho V^2) - \rho g \sin\theta - \frac{\tau \pi d}{A_P} \qquad (3.8)$$

$$\frac{dP}{dL} = -\frac{d}{dL}(\rho V.V) - \rho g \sin\theta - \frac{\tau \pi d}{A_P} \qquad (3.9)$$

$$\frac{dP}{dL} = -\rho V \frac{d}{dL}(V) - V\frac{d}{dL}(\rho V) - \rho g \sin\theta - \frac{\tau \pi d}{A_P} \quad (3.10)$$

Substituting equation 3.5 into the equation 3.10

$$\frac{dP}{dL} = -\rho V \frac{d}{dL}(V) - \rho g \sin\theta - \frac{\tau \pi d}{A_P} \quad (3.11)$$

Kinetic energy = $\frac{1}{2} * \text{mass} * (\text{velocity})^2 = \text{force} * \text{distance}$

kinetic energy = $\frac{1}{2} * \text{mass} * (\text{velocity})^2 = \text{pressure} * \text{Volume}$

Kinetic energy = $\frac{1}{2} * \rho V^2 = P$, substituting into equation (3)

$$\rho V \frac{\mathbf{d}}{\mathbf{dL}}\left(e + \frac{P}{\boldsymbol{\rho}}\right) = -\rho V . V\frac{dV}{dL} - \rho V g \sin\theta - \frac{q \pi d}{A_p} \quad (3.12)$$

Using the definition of enthalpy, $h = u + PV$

Where $internal\ energy\ per\ unit\ mass = u = e$

$$h = e + PV \quad (3.13)$$

Specific volume, $V = 1/\rho$ (3.14)

$$h = e + \frac{P}{\rho} \quad , \quad (3.15)$$

$\frac{dh}{dL} = \frac{d}{dL}\left(e + \frac{P}{\rho}\right)$, multiplying each term by ρV (3.16)

$\rho V \frac{dh}{dL} = \rho V \frac{d}{dL}\left(e + \frac{P}{\rho}\right)$, this is similar to equation (5), hence (3.17)

$$\rho V \frac{dh}{dL} = \rho V \frac{d}{dL}\left(e + \frac{P}{\rho}\right) = -\rho V . V\frac{dV}{dL} - \rho V g \sin\theta - \frac{q \pi d}{A_p} \quad (3.18)$$

Dividing both side by $\boldsymbol{\rho V}$,

$$\frac{dh}{dL} = -V\frac{\mathbf{dV}}{\mathbf{dL}} - g \sin\theta - \frac{\mathbf{q \pi d}}{\mathbf{W}} \quad (3.19)$$

Where mass flow rate, $w = \rho V A_P$ (3.20)

The heat transfer to the surroundings can be determined by use of the concept of overall heat transfer coefficient, U:

$$q = U(T - Te) \tag{3.21}$$

The geometrical configuration of the wellbore or pipeline and all the heat-transfer mechanism involved should be considered carefully in the determination of U.

$$U = \frac{1}{r}\left[\frac{1}{U_0} + \frac{f(t)}{K_e}\right]^{-1} \tag{3.22}$$

For wellbore temperature prediction, the first term inside the parenthesis accounts for the heat transfer mechanisms in the wellbore itself, while the second term accounts for the transient heat transfer in the reservoir.

For pipeline temperature prediction, the first term inside the bracket is usually considered.

Substituting (7) into (6)

$$\frac{dh}{dL} = -V\frac{dV}{dL} - g\sin\theta - \frac{U\pi d}{W}(T - Te) \tag{3.23}$$

From first law of thermodynamics, which state that energy can neither be created nor destroyed during a process, it can only change forms.

$$\Delta U = q + w \tag{3.24}$$

In differential form,

$$du = dq + dw \tag{3.25}$$

But $dw = -pdv$ (3.26)

$$du = dq - pdv \tag{3.27}$$

Choosing internal energy to be a function of T and V, that is

$u = u(T, V)$, taking its total differential form

$$du = \left[\frac{\partial u}{\partial T}\right]_V dT + \left[\frac{\partial u}{\partial V}\right]_T dV \tag{3.28}$$

At constant volume, $dV = 0$, which implies that, $du = dq$

$$du = \left[\frac{\partial u}{\partial T}\right]_V dT = C_V dT \tag{3.29}$$

$$C_V = \left[\frac{\partial u}{\partial T}\right]_V \tag{3.30}$$

$$C_V = \left[\frac{\partial q}{\partial T}\right]_V \tag{3.31}$$

Applying same manner for enthalpy changes,

$$h = u + pv \tag{3.32}$$

$$dh = du + d(pv) \tag{3.33}$$

$$dh = du + pdv + vdp \tag{3.34}$$

$$\text{recall that } du = dq - pdv \tag{3.35}$$

$$\text{hence } dh = dq - pdv + pdv + vdp \tag{3.36}$$

$$dh = dq + vdp \tag{3.37}$$

Choosing enthalpy to be a function of T and P, that is, $h = h(T, P)$

$$dh = \left[\frac{\partial h}{\partial T}\right]_P dT + \left[\frac{\partial h}{\partial P}\right]_T dP \tag{3.38}$$

Using the definition of $C_P = \left[\frac{\partial h}{\partial T}\right]_P$, we have

$$dh = C_P dT + \left[\frac{\partial h}{\partial P}\right]_T dP \tag{3.39}$$

Evaluating the enthalpy gradient in terms of temperature and pressure gradients:

$$dh = C_P \frac{dT}{dL} + \left[\frac{\partial h}{\partial P}\right]_T \frac{dP}{dL} \tag{3.40}$$

Applying Joule Thomson coefficient, η

$$\eta = \left[\frac{\partial T}{\partial P}\right]_h = \frac{\left[\frac{\partial h}{\partial P}\right]_T}{\left[\frac{\partial h}{\partial T}\right]_P} \tag{3.41}$$

$$\eta \left[\frac{\partial h}{\partial T}\right]_P = \left[\frac{\partial h}{\partial P}\right]_T \tag{3.42}$$

$$\eta C_P = \left[\frac{\partial h}{\partial P}\right]_T \quad (3.43)$$

$$\frac{dh}{dL} = C_P \frac{\partial T}{\partial L} - \eta C_P \frac{\partial P}{\partial L} \quad (3.44)$$

Equating equation (9) and (10) gives

$$C_P \frac{\partial T}{\partial L} - \eta C_P \frac{\partial P}{\partial L} = -V\frac{\mathbf{dV}}{\mathbf{dL}} - g\sin\theta - \frac{\mathbf{U\pi d}}{\mathbf{w}}(T - Te) \quad (3.45)$$

Re-writing equation (11)

$$\frac{dT}{dL} + \frac{U\pi d}{wC_P}T = \frac{U\pi d}{wC_p}T_e + \frac{1}{C_P}\left[\eta C_P \frac{dP}{dL} - g\sin\theta - v\frac{dv}{dL}\right] \quad (3.46)$$

Defining [8] a relaxation distance, A, as

$$A = (wC_P/U\pi d) \quad (3.47)$$

And a dimensionless parameter, $\mathbf{\Phi}$, as

$$\Phi = \left[\rho\eta C_P \frac{dP}{dL} - \rho g\sin\theta - \rho v\frac{dv}{dL}\right] \Big/ \frac{dP}{dL} \quad (3.48)$$

Re-writing equation (12)

$$\frac{dT}{dL} + \frac{1}{A}T = \frac{1}{A}T_e + \frac{1}{\rho C_P}\frac{dP}{dL}\Phi \quad (3.49)$$

Only mathematical manipulation has been done to the enthalpy equation, and the analysis has been carried out rigorously without simplification. Now, with the assumption that the surrounding temperature is a linear function of depth, it can be expressed as

$$T_e = T_{ei} - g_e L\sin\theta \quad (3.50)$$

Substituting equation (16) into equation (15) gives

$$\frac{dT}{dL} + \frac{1}{A}T = \frac{1}{A}T_{ei} - \frac{1}{A}g_e L\sin\theta + \frac{1}{\rho C_P}\frac{dP}{dL}\mathbf{\Phi} \quad (3.51)$$

From $\frac{dy}{dx} + Py = Q$

Integrating factor, $IF = e^{\int P dx}$

Total solution is $y.IF = \int Q.IF\,dx$

if for a certain segment of the pipe, $U, C_P, \eta, g_e, \theta, \mathbf{v}\frac{\mathbf{dv}}{\mathbf{dL}}$, and $\frac{\mathbf{dP}}{\mathbf{dL}}$, Can be considered approximately constant, eq. 17 can be integrated using the above integrating process, yielding an explicit equation for the temperature.

$IF = e^{\int \frac{dL}{A}}$, hence $IF = e^{\frac{L}{A}}$

Total solution becomes $$T.e^{\frac{L}{A}} = \int \left(\frac{1}{A}T_{ei} - \frac{g_e}{A}L\sin\theta + \frac{1}{\rho C_P}\frac{dP}{dL}\Phi\right)e^{\frac{L}{A}}\,dL \quad (3.52)$$

$$T.e^{\frac{L}{A}} = \int_0^L \frac{1}{A}T_{ei}e^{\frac{L}{A}} - \int_0^L \frac{g_e}{A}L\sin\theta e^{\frac{L}{A}}\,dL + \int_0^L \frac{1}{\rho C_P}\frac{dP}{dL}\Phi \mathbf{e}^{\frac{L}{A}}dL \quad (3.53)$$

$$= \frac{T_{ei}Ae^{\frac{L}{A}}}{A} - \frac{g_e}{A}\sin\theta \int Le^{\frac{L}{A}}dL + \frac{1}{\rho C_P}\frac{dP}{dL}\Phi \int_0^L \mathbf{e}^{\frac{L}{A}}\,dL \quad (3.54)$$

$$= \left(T_{ei}e^{\frac{L}{A}} - T_{ei}\right) - \left(g_eL\sin\theta\, e^{\frac{L}{A}} - 0\right) + \left(g_eA\sin\theta e^{\frac{L}{A}} - g_eA\sin\theta\right) +$$

$$\left(\frac{1}{\rho C_P}\Phi A\frac{dP}{dL}e^{\frac{L}{A}} - \frac{1}{\rho C_P}\Phi A\frac{dP}{dL} + Const.\right) \quad (3.55)$$

recall $T_e = T_{ei} - g_eL\sin\theta$

when $L = 0, T_e = T_{ei}$ and $T = T_i$

Substituting $L = 0$ into Eq. 17a, yields Const, $C = T = T_i$

$$T = \left(T_{ei}e^{\frac{L}{A}} - T_{ei}\right) - \left(g_eL\sin\theta\, e^{\frac{L}{A}} - 0\right) + \left(g_eA\sin\theta e^{\frac{L}{A}} - g_eA\sin\theta\right) + \left(\frac{1}{\rho C_P}\Phi A\frac{dP}{dL}e^{\frac{L}{A}} - \frac{1}{\rho C_P}\Phi A\frac{dP}{dL}\right) + T_i \quad (3.56)$$

$$T = \left(T_{ei} - T_{ei}e^{\frac{-L}{A}}\right) - (g_eL\sin\theta) + \left(g_eA\sin\theta - g_eA\sin\theta\, e^{\frac{-L}{A}}\right) + \left(\frac{1}{\rho C_P}\Phi A\frac{dP}{dL} - \frac{1}{\rho C_P}\Phi A\frac{dP}{dL}e^{\frac{-L}{A}} + T_ie^{\frac{-L}{A}}\right) \quad (3.57)$$

$$T = (T_{ei} - g_e L \sin\theta) + (T_i - T_{ei})e^{\frac{-L}{A}} + g_e A \sin\theta\left(1 - e^{\frac{-L}{A}}\right) + \frac{1}{\rho C_P}\Phi A \frac{dP}{dL}\left(1 - e^{\frac{-L}{A}}\right) \quad (3.58)$$

The temperature equation above is originally developed by Alves et al[1]. The equation was modified in this work as shown below.

$$\tilde{\eta} = -\frac{1}{w\widehat{C_P}}\left\{\frac{w_g}{\rho_g}\left[-\frac{T}{Z}\left(\frac{\partial Z}{\partial T}\right)_P\right] + \frac{w_L}{\rho_L}\right\} \quad (3.59)$$

From Sutton's correlation for z factor

$$Z = \frac{2.7P\delta_g}{\rho T} \quad (3.60)$$

$$\rho = \frac{2.7P\delta_g}{ZT} \quad (3.61)$$

$$\left(\frac{\partial Z}{\partial T}\right)_P = -\frac{2.7P\delta_g}{\rho T^2} \quad (3.62)$$

Substituting the differential of Z-factor with respect to temperature at constant pressure, and also the equation for the density of gas into the average Joule Thompson coefficient, it becomes

$$\tilde{\eta} = -\frac{1}{w\widehat{C_P}}\left\{\frac{2.7Pw_g\delta_g}{TZ(\rho_g)\text{^}2} + \frac{w_L}{\rho_L}\right\} \quad (3.63)$$

The joule Thomson coefficient above, Is no more a function of the differential of the Z-factor with respect to temperature as was derived in the Alves et al joule Thomson coefficient, but now a function of the mass flow rate of the individual phases of the fluid.

The above equation is substituted into the dimensionless parameter

$$\Phi = \left[\rho\eta C_P \frac{dP}{dL} - \rho g \sin\Theta - \rho v \frac{dv}{dL}\right] / \frac{dP}{dL} \quad (3.64)$$

$$T = (T_{ei} - g_e L \sin\theta) + (T_i - T_{ei})e^{\frac{-L}{A}} + g_e A \sin\theta\left(1 - e^{\frac{-L}{A}}\right) + \frac{1}{\rho C_P}\Phi A \frac{dP}{dL}\left(1 - e^{\frac{-L}{A}}\right) \quad (3.65)$$

3.4 APPROXIMATION FOR BLACK OIL MODEL

A black oil model's validity resets on the assumption that the hydrocarbon mixture is composed of only two components (denoted oil and gas), each with a fixed composition. The gas is said to be dissolved in the oil, with amount of dissolved gas decreasing with decreasing pressure. The oil component in the pipeline generally is defined as stock-tank oil. A black oil model usually treats PVT properties (solution gas, densities, and viscosities) as single value functions of pressure.

The total enthalpy of a mixture for two phase flow systems is the sum of the individual phases. Thus neglecting the effect of mass transfer, the enthalpy gradient can be written as

$$w\frac{dh}{dL} = w_g\frac{dh_g}{dL} + w_L\frac{dh_L}{dL} \tag{3.66}$$

$$\frac{dh}{dL} = \frac{w_g}{w}\frac{dh_g}{dL} + \frac{w_L}{w}\frac{dh_L}{dL} \tag{3.67}$$

The enthalpy gradient for each phase is given by

$$\frac{dh_g}{dL} = -\eta_g C_{pg}\frac{dP}{dL} + C_{pg}\frac{dT}{dL} \tag{3.68}$$

$$\frac{dh_L}{dL} = -\eta_L C_{pL}\frac{dP}{dL} + C_{pL}\frac{dT}{dL} \tag{3.69}$$

$$\text{where } \eta_g = \frac{1}{C_{pg}}\left\{T\left[\frac{\partial}{\partial T}\left(\frac{1}{\rho_g}\right)\right]_p - \frac{1}{\rho_g}\right\} \tag{3.70}$$

$$\text{and } \eta_L = \frac{1}{C_{pL}}\left\{T\left[\frac{\partial}{\partial T}\left(\frac{1}{\rho_L}\right)\right]_p - \frac{1}{\rho_L}\right\} \tag{3.71}$$

Using the thermodynamic behavior of a real gas and assuming liquid as incompressible yields

$$\eta_g = \frac{1}{C_{pg}\rho_g}\left[-\frac{T}{Z}\left(\frac{\partial Z}{\partial T}\right)_p\right] \tag{3.72}$$

$$\eta_L = \frac{-1}{C_{PL}\ \rho_L} \tag{3.73}$$

Substituting Eq. 25 into Eq. 21 and Eq. 26 into Eq. 22, it becomes

$$\frac{dh_g}{dL} = \frac{1}{\rho_g}\left[-\frac{T}{Z}\left(\frac{\partial Z}{\partial T}\right)_p\right]\frac{dP}{dL} + C_{pg}\frac{dT}{dL} \tag{3.74}$$

$$\frac{dh_L}{dL} = \frac{1}{\rho_L}\frac{dP}{dL} + C_{pL}\frac{dT}{dL} \quad (3.75)$$

Substituting Eq. 27 and 28 into Eq. 20 yields

$$\frac{dh_L}{dL} = \frac{w_g}{w}\left\{\frac{1}{\rho_g}\left[-\frac{T}{Z}\left(\frac{\partial Z}{\partial T}\right)_P\right]\frac{dP}{dL} + C_{pg}\frac{dT}{dL}\right\} + \frac{w_L}{w}\left(\frac{1}{\rho_L}\frac{dP}{dL} + C_{pL}\frac{dT}{dL}\right) \quad (3.76)$$

Rearranging Eq. 29 gives

$$\frac{dh_L}{dL} = \frac{w_g c_{Pg} + w_L c_{PL}}{w}\frac{dT}{dL} + \frac{1}{w}\left\{\frac{w_g}{\rho_g}\left[-\frac{T}{Z}\left(\frac{\partial Z}{\partial T}\right)_P\right] + \frac{w_L}{\rho_L}\right\}\frac{dP}{dL} \quad (3.77)$$

The average heat capacity for two-phase mixture is

$$\widetilde{C_P} = \frac{(w_g C_{Pg} + w_L C_{PL})}{w} \quad (3.78)$$

$$\text{Where } C_{PL} = \left(\frac{q_o}{q_o + q_w}\right)c_{po} + \left(1 - \frac{q_o}{q_o + q_w}\right)c_{pw} \quad (3.79)$$

And average Joule Thomson coefficient becomes

$$\tilde{\eta} = -\frac{1}{W\widetilde{C_P}}\left\{\frac{w_g}{\rho_g}\left[-\frac{T}{Z}\left(\frac{\partial Z}{\partial T}\right)_P\right] + \frac{w_L}{\rho_L}\right\} \quad (3.80)$$

$$\text{where } w_L = \frac{(q_w\delta_w + q_o\delta_o)}{246.6} \quad (3.81)$$

$$\text{where } w_g = \frac{q_g\delta_g}{1130900} \quad (3.82)$$

$$W = W_L + W_g \quad (3.83)$$

$$\text{Or } \tilde{\eta} = -\frac{1}{\rho_n\widetilde{C_P}}\left\{y_g\left[-\frac{T}{Z}\left(\frac{\partial Z}{\partial T}\right)_P\right] + y_L\right\} \quad (3.84)$$

For single phase fluid, $y_g = 0, y_L = 1, \rho_n = \rho_L$ and Eq. 33 become the same as Eq. 26 for an incompressible fluid. Also, for single phase gas, $y_g = 1. y_L = 0, \rho_n = \rho_g$ and Eq. 33 become the same as Eq. 25 for real gas.

The heat capacity of a real gas does not vary much over a broad range of temperatures. Thus, average value for $\widetilde{C_P} = 0.65\frac{Btu}{Ibm-°F}$ is used.

3.5 CALCULATION PROCEDURE

In this study, we applied the unified and simplified model in generating the temperature profile in the wellbore. The pressure gradient in this model is a function of the average pressure and temperature of the pipe segment. Thus an iterative procedure is required for this calculation, the "average temperature and Z-factor method is used to determine the average pressure and temperature which requires at most four iterations for perfect convergence.[17] an excel sheet was created for this iteration.

The gas compressibility, z-factor is determined using Sutton's correlation from the known fluid composition for the buttomhole depth and Lee et al correlation was used as depth progresses up. The density of the gas was also determined using the Lee et al correlation[18]

The no- slip density, mixture or slip density etc was determined from Beggs and Brill correlation which are imputed into the Beggs and Brill multiphase flow equation.[16]

The dead oil viscosity and oil viscosity, gas viscosity, gas solubility are determined using Beggs- Robinson correlation, Lee et al correlation, and Glaso correlation, respectively.[18]

The oil viscosity obtained is imputed into the Beggs and Brill pressure gradient equation. The joule Thomson coefficient is dependent on the average temperature and the mass flow rate of each phases which is calculated into the dimensionless parameter (Φ) and then into the model equation. The overall heat transfer coefficient is varied and 2.7 is used below sea level and 2.8 above the sea level for the calculation of the relaxation distance.

Summarized steps of parameter calculations are found in the appendix.

3.6 VALIDATION OF THE ANALYTICAL MODEL

The model equation above is validated by using the model equation to produce the same work done by Alves et al[1], the only difference done by this research work is the modification of the joule Thomson coefficient which is explained in the model derivation in chapter 3. *This research work also assume an*

overall heat transfer coefficient of 2.7 below sea bed and 2.8 above sea bed, which is quite different from that of Alves with 2 as overall heat transfer coefficient above sea bed and 1 below sea bed. The result obtained for by the model equation is shown below in figure 3.1.The fluid composition, operational conditions, and overall heat transfer coefficients etc. used in found in reference, 1.

3.6.1 TEMPERATURE PROFILE FOR TWO PHASE FLOW MODEL (liquid and gas)

The calculation procedure is well elaborated in the appendix, equations for two phase flow and three phase flow are shown. The result as shown in figure 3.1 is same as that of Alves but with different overall heat transfer coefficient as explained above.

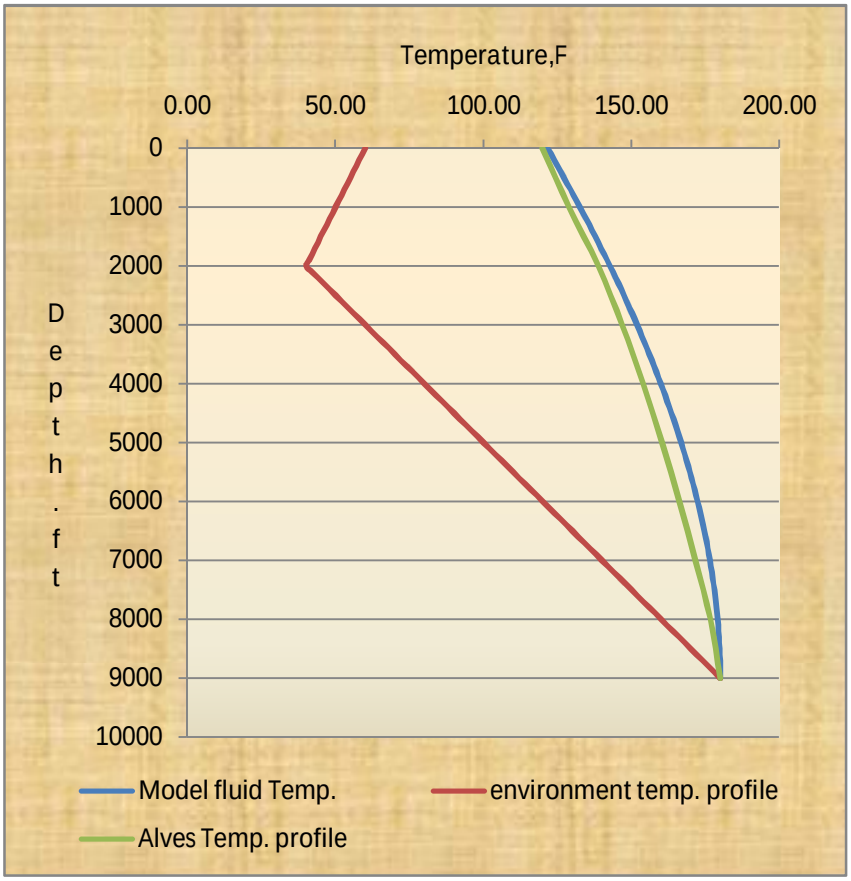

	Alves	Model
Depth(ft)	Temp(oF)	
0	120	121.6
1000	128.99	132.6
2000	138.81	142.8
3000	146.93	151.8
4000	154.01	159.9
5000	160.37	166.7
6000	166.2	172.3
7000	171.6	176.5
8000	176.67	179.1
9000	180	180

Figure 3.2 temperature profile for two phase liquid and gas production

CHAPTER FOUR

ANALYSIS AND INTERPRETATION

Understanding the influence of geothermal gradient and thermal processes in fluid flowing in the reservoir and wellbore is very important for a meaningful interpretation of the acquired down-hole data from the model. Temperature changes in the wellbore occur comparatively to the geothermal temperature profile.

Generally, temperature changes are caused by flow friction in the reservoir, Joule Thomson -cooling for gas and in most cases, heating for oil and water, elevation changes in the wellbore and geothermal gradient in the subsurface. Inflow fluid is expected to enter the well from the reservoir at the geothermal temperature at the entry depth. This fluid undergoes Joule Thomson cooling or heating in the near wellbore due to pressure drop and mixes with other inflow fluid as it flows up the wellbore. It is found that the resulting well stream temperature is directly related to the percentage of each inflow zone distribution and also the fluid type at the inflow location. Hence for correct interpretation, care should be taken to ensure the accuracy of the fluid properties because the temperature changes are sensitive to contrast in reservoir fluid properties at each phase. Pressure profile are less sensitive to flow dynamics than temperature profiles, nevertheless, pressure profiles corroborates the temperature trend analysis for different flow conditions, (Dawkrajai 2006, Vander Steen 2006).

When oil and water are produced from the same depth, oil warms up (viscous dissipative heating) faster than water because of different thermal properties and therefore enters the wellbore with a higher temperature. In this scenario, the water enters with a lower temperature and cools the temperature profile. However, when a well produces water by water coning from warmer aquifer below production zone, a warming effect and associated high entry temperature is encountered. Exothermic reaction of the cement sidetrack plug is known to cause an increase in the wellbore temperature profile.

Beside the fluid type, pressure drawdown is another factor that control Joule Thomson behavior of inflow fluids. Small frictional heating can be expected for a high rate (high permeability) reservoirs since the pressure drawdown is often small while high frictional heating occurs in the reservoir with large drawdown even if the flow rate is low. High pressure drawdown yields high Joule Thomson heating (Brown 2006, Pinzon et al.2007). At very high pressures, gas exhibits warm joule Thomson effect. This may be attributed to the change in gas properties into liquid properties as the gas is compressed under high pressure.

To discern flow contribution, detect gas, oil or water inflow zones and to locate contributing sections along the wellbore, we need to look for deviation of the thermal profile of the well when compared with geothermal temperature baseline. These anomalous deviations depict trend that can be analyzed and interpreted to yield useful well information that subsequently form the basis for production optimization and well control. The geothermal baseline can be obtained from field temperature database or by shutting in the well and acquiring stabilized down-hole temperature data.

Slope changes which usually occur at inflow sections identify the producing zones from non-producing zones and sometimes can be used to mark the inflow boundary of one fluid from another fluid along the wellbore.

4.1 RESULT AND DISCUSSION

Using the model described above, we generated temperature and pressure profiles for single- phase oil flow, two-phase oil water flow, two phase oil gas and three-phase oil water and gas flow to a 40 degree inclined well to the vertical or 50 degree inclined well to the horizontal. Using this profile, we detected the inflow of water and gas entry into the wellbore. Three cases are presented to illustrate the application of the model. The effect of water entry was shown which explains the consequence of warmer water entry as a result of water coning from a deeper zone, effect of gas entry on temperature

profile, and sensitivity of temperature profile to ratio of water to gas inflow or production. We use fluid properties correlations presented in Appendix A. the parameters of the analytical model are summarized in Tables 4.1 and 4.2.

Table 4.1 INPUTS FOR WELLBORE PARAMETERS AND OPERATIONAL CONDITIONS

Gauge measure depth, ft	4543.11
True vertical depth, ft	3491.41
Inclination of pipe from vertical, deg	40
Environment thermal gradient,°F/ft	0.02
Tubing ID, in	2.992
Sea water level, ft	60
Well true vertical depth below seabed, ft	4483.11
Bottomhole pressure, psia	1557.3
Buttomhole temperature, °F	152

TABLE 4.2 INPUTS FOR FLUID PROPERTIES

OIL	
Density at surface, lbm/ft^3	57.55858
Density at reservoir, lbm/ft^3	52.7513
Heat capacity, Btu/lbm-°F	0.53
Viscosity, cp	2.85
Formation volume factor, RB/STB	1.12
WATER	
Density, lbm/ft^3	62.43
Heat capacity, Btu/lbm-°F	1
GAS	
Gas gravity	0.65
Heat capacity, Btu/lbm-°F	0.5

4.1.1 TEMPERATURE PROFILES FOR SINGLE PHASE OIL PRODUCTION

The section shows the temperature profiles for a case of oil inflow alone in the well. Although the direct way of to infer the inflow rate profile is the pressure profiles from a pressure-based productivity model. It is assumed that the geothermal temperature at the well depth is known and the fluid inflow into the wellbore starts at the geothermal temperature.

For oil, figure 4.1 shows the temperature profile for a single oil production at a flow rate of 4000 bbl/day. The temperature at the pipe intake is assumed to be the same with the geothermal temperature which explains why the environmental temperature profile and fluid temperature starts

at the same temperature. All of the temperatures as the fluid flows upward are greater than the geothermal temperature because the oil expands as pressure drops, and gains temperature due to Joule Thomson effect (Joule Thomson heating). The surface temperature is 138.9 **°F,** the temperature range from the above profile is 152-138.9 **°F.** There is a slight deviation of the fluid temperature from the geothermal temperatures but fluid temperature shows a decreasing trend or a change of slope as it flows upward.

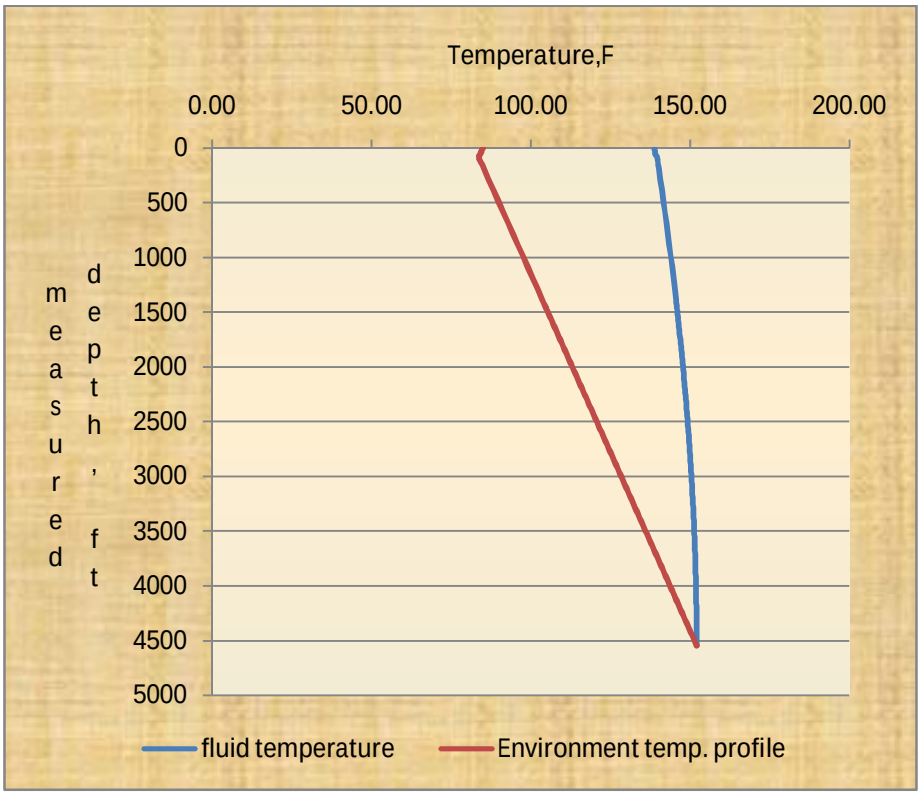

Depth(ft)	Temp(^{o}F)
0	138.9
583	142.2
1083	144.4
1573	146.3
2023	147.8
2503	149.2
3013	150.4
3523	151.3
4003	151.8
4543	152

Figure 4.1 temperature profiles for single phase oil production

4.1.2 TEMPERATURE PROFILES FOR 2-PHASE OIL AND GAS INFLOW (GAS ENTRY EFFECT)

When gas is produced, wellbore usually experienced temperature cooling. As the pressure decreases, the gas expands and the temperature decrease because of Joule Thomson cooling, the temperature profile as shown in fig 4.3 shows more significant anomalies when compared to that of oil production temperature profile. The surface temperature from the profile is 136.7 **°F** which is lower than that of oil, the temperature range is **152-136.7 °F**.

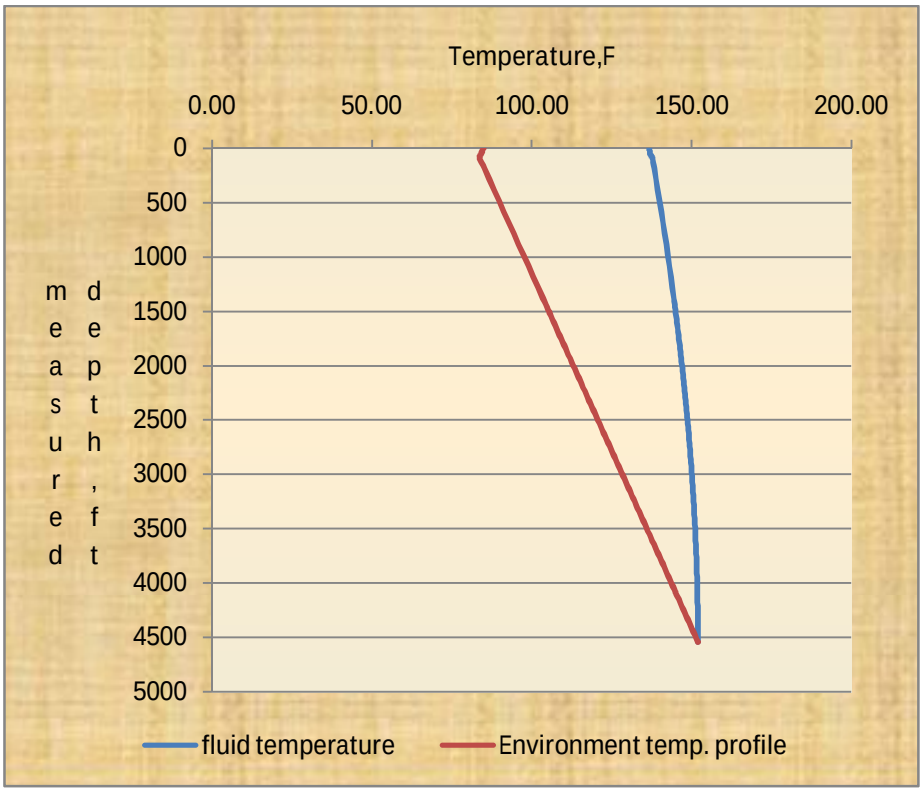

Depth(ft)	Temp(^{o}F)
0	136.7
583	140.5
1083	143.1
1573	145.3
2023	147.1
2503	148.7
3013	150.1
3523	151.2
4003	151.8
4543	152

Figure 4.3 Temperature profile for fluid production with gas entry effect

4.1.3 TEMPERATURE PROFILES FOR 3-PHASE OIL, GAS AND WATER INFLOW (WATER ENTRY EFFECT)

For water, as shown in fig 4.2, shows similar plot to that of oil production but the size of temperature change is smaller than for oil because water has a greater heat capacity and density, so the Joule Thomson effect for water is smaller than for oil. Also, water has a larger heat viscosity than oil at reservoir condition (152 °F, 1557 psia) so the water flow rate is less than that of oil rate under the same drawdown pressure. Water entry also slows down temperature decline, it may be attributed to inflow of water from a warmer water entry zone as a result of water flow from a warmer aquifer below the producing zone (water coning).

It has often been said entering water has warmer temperature than oil because water is produced from a deeper zone than due to water coning. But we assume that the inflow temperature is only a function of wellbore depth and surrounding temperature is a linear function of the wellbore depth, hence temperature of fluid at pipe intake is assumed to be equivalent to the environmental temperature at the buttom hole. On the temperature plot as shown in figure 4.2, the surface temperature is 139.81 °F which is higher than the surface temperature (138.9°F) for singe phase oil production, the temperature range is 152-139.8 °F.

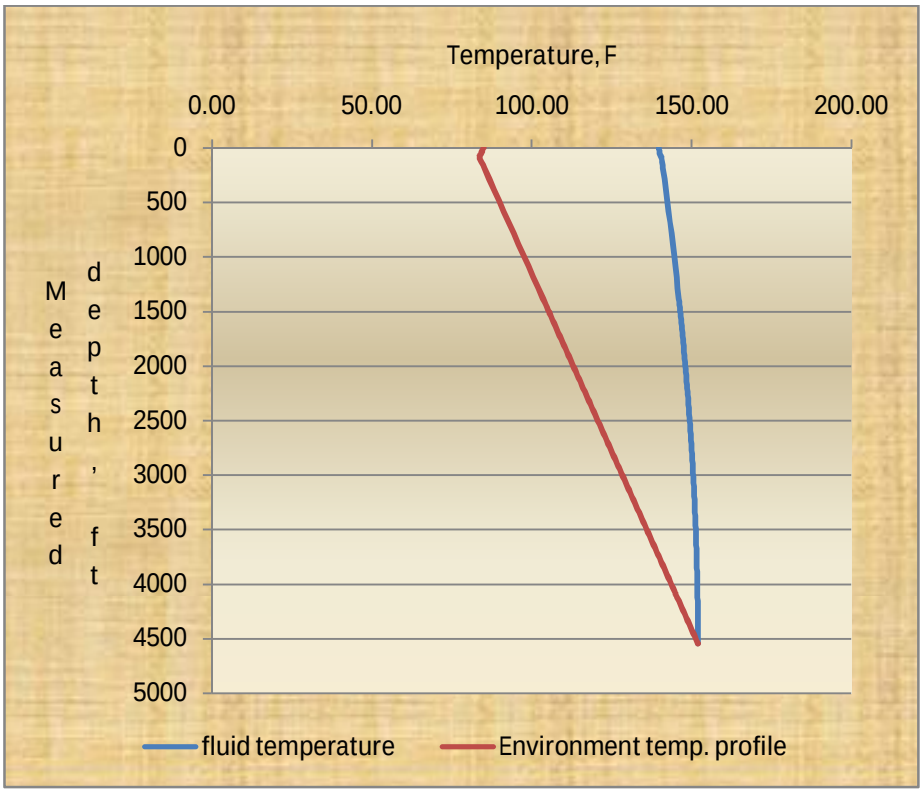

Depth(ft)	Temp(^{o}F)
0	139.1
583	142.3
1083	144.5
1573	146.4
2023	147.9
2503	149.3
3013	150.5
3523	151.3
4003	151.8
4543	152

Figure 4.2 Temperature profile for fluid production with water entry effect

4.1.4 TEMPERATURE PROFILE COMPARISON FOR THE SINGLE PHASE, 2- PHASE AND 3-PHASE CASES ABOVE

it can be seen that the profile with water entry effect the highest temperature at the surface which tells that water entry causes an increase in temperature. Also the least temperature profile is that of gas which indicates that gas entry causes a decrease in temperature due to Joule Thomson cooling.

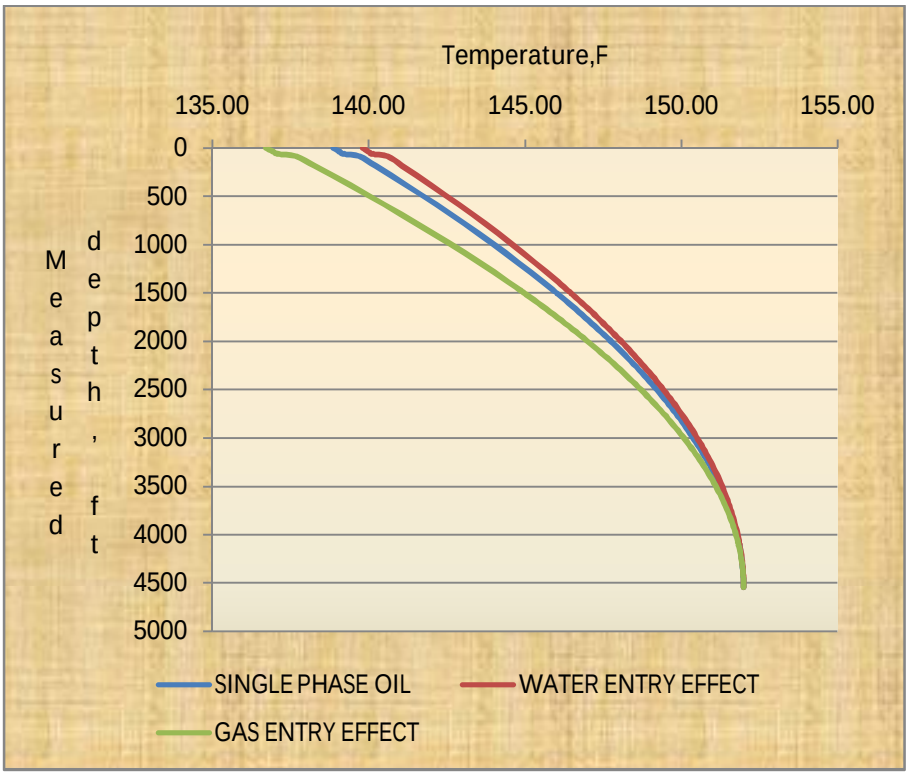

Figure 4.5 Temperature profile comparison for single phase oil, 2-phase (oil and gas), and 3-phase (oil, gas and water flow)

CHAPTER FIVE

CONCLUSION AND RECOMMENDATIONS

In this study, we used the model developed to predict temperature behavior along the well in the inclined section of the horizontal well at 50 degree to the horizontal to show the application using the temperature profiles to detect, locate, and analyze the effect of water and gas entry in oil producing well. The cases showed increasing temperature profile due to water entry as a result of water entry from warmer aquifer, decrease temperature profile due to gas entry. A study was also shown to investigate the effect of flow rate especially on the water temperature profile. From the study, we found

5.1 CONCLUSIONS

a. Temperature prediction model for predicting flowing temperature in wellbores and pipelines was developed. The model is general and unified and can be applied to producing or injection wells over the entire inclination angle range, from horizontal to vertical, with compositional and black-oil models.
b. For single phase oil production, the overall temperature changes are small compared to that of gas.
c. In general, gas production causes a temperature decrease due to Joule Thomson effect.
d. Temperature increase is due to water entry as a result of water coning.
e. The model can be used to model the amount of gas or water influx into the wellbore.
f. Predicting water and gas inflow in wellbores and pipelines enhances production optimization in effective planning of surface equipment.

5.2 RECOMMENDATION

This study is only intended to establish a fundamental understanding of the temperature behavior under specific cases. A more advanced and detail modeling could be further done as follows.

a. Temperature prediction model to detect and locate wax deposition in the wellbore.

b. Prediction of emulsion formation from temperature profile.

c. Temperature prediction model for three-phase in unsteady state flow process.

d. Predicting large permeability zones form in the reservoir from temperature profiles.

NOMENCLATURE

Symbol	Description
A	thermal relaxation distance, L
A_P	cross-sectional area of pipe, L, ft^2
C_P	heat capacity at constant pressure, L^2/t^2T, $\frac{Btu}{lbm-°F}$
d	pipe diameter, L, ft^2
e	internal energy per unit of mass, L^2/t^2
f(t)	dimensionless transient heat conduction time function for earth
g	gravitational acceleration, L/t^2, ft-lbm/sec^2-lbf
g_e	environmental thermal gradient, T/L, $^oF/ft$
h	enthalpy per unit mass, L^2/ft^2
K_e	thermal conductivity of earth, mL/t^3T, Btu/D-ft-^oF
L	length, L, ft
P	pressure, m/Lt^2, psi
q	heat flow, m/t^2
q_o	oil flow rate, STB/D
q_w	water flow rate, STB/D
q_g	gas flow rate, Scf/D
r	radius, L, ft
T	temperature, T, ^oF
T_e	temperature of environment, T, ^oF
T_{ei}	temperature of environment at pipe intake, T, ^oF
T_i	temperature at pipe intake, T, ^oF

U	overall heat-transfer coefficient, m/t^3T, Btu/(hr-ft^2- ^oF)
U_O	overall heat transfer coefficient times pipe radius, mL/t^3T, Btu/(hr-ft^2- ^oF)
V	velocity, L/t, ft/sec
W	mass flow rate, m/t, lbm/sec
y	no-slip hold up
Z	gas compressibility factor
ρ_M	slip or mixture density, m/L^3, (lbm/ft3)
$\boldsymbol{\theta}$	Inclination angle with horizontal
P	density, m/L^3, (lbm/ft3)
ρ_n	no-slip density, m/L^3, (lbm/ft3)
τ	shear stress at pipe wall, m/Lt^2
$\boldsymbol{\Phi}$	dimensionless correction parameter
$\boldsymbol{\gamma}$	gravity
$\boldsymbol{\mu}$	viscosity, cp
P_{Pr}	pseudoreduced pressure
T_{Pr}	pseudoreduced temperature
P_{PC}	pseudo-critical pressure, m/Lt^2, psi
T_{PC}	pseudo-critical temperature, T, ^oF

Subscripts

g	gas
L	liquid

Superscripts

–	average

REFERENCES

1. Alves, I.N., Alhanatl, F.J.S., Shoham, O.: "A unified model for predicting flowing temperature distribution in wellbores and Pipelines". SPE Prod. Eng. 20632, 363– 367. (Nov. 1992).
2. James, J.S. Alex, V.S.: "Distributed temperature sensing-A DTS primer for oil and gas production". (May 2003).
3. Leksono, M., Michael A.:"A compositional two phase flow model for analyzing and designing complex pipeline network systems". (June 1990).
4. Beggs, H.D., Brill, J.P.: "A study of two – phase flow in inclined pipes". (May 1973).
5. Gould, T.L.: "Compositional two phase flow in pipelines". JPT (March 1979) 373-84 : Trans.,AIME,267
6. Pinan D.: "Temperature prediction model for a producing horizontal well". (Aug. 2006).
7. Yunus, A.C.,Michael, A.B.: *Thermodynamics –An engineering approach*. Fifth edition.
8. Rameh, H.J. Jr.: "Wellbore heat transmission" JPT (April 1962) 427-35:Trans.,AIME,225
9. Zhuoyi, L., Ding, Z.: "Predicting flow profile of horizontal well by downhole pressure and DTS data for water-drive reservoir". SPE Prod. Eng. 124873. (Oct. 2009).
10. Yoshioka, K., Zhu D., Hill. A.D.: "A new inversion method to interpret flow profiles from distributed temperature and pressure measurements in horizontal wells". (Nov. 2007).
11. Ochi, I.A., Zhuoyi, L., Zhu, D., Hill, A.D.: "An interpretation method of downhole temperature and pressure data for flow profiles in gas wells". (Oct. 2008).
12. Octavio, C., Mario, A.V.: "Prediction of pressure, temperature, and velocity distribution of two phase flow in oil wells." Journal of petroleum science and technology 46 (Dec. 2005) 195-208.
13. Jacques, H.: "Ramey's wellbore heat transmission revisited". (Dec. 2004).

14. Yoshioka, K., Zhu, D., Hill, A.D.: “Dawkrajai, P., Lake, L.W. “Detection of water or gas entries in horizontal wells from temperature profiles”. (April 2006).

15. Hani, E., Magdy, S.O., Mahmut, S.: “Use of temperature data in gas well test”. (Oct. 1999).

16. Brill, J.P., Hemanta, M.: *Multiphase flow in wells.* (1999).

17. Lee, J., Robert, A.W.: *Gas reservoir engineering*. (1996).

18. Tarek, A.: *Reservoir engineering hand book second edition.* (2000).

19. Rajiv, S., Dorty, D.R., Zellmir S.: “Predicting temperature profiles in a flowing well”. (Nov 1991).

APPENDIX A

FLUID PROPERTIES

The objective of this appendix is to show the following steps that make up the procedure for using the simplified model. There are many empirical correlations based on laboratory PVT analyses in the literature. We choose correlations that can be applied to the oil field ranges of temperature and pressure. The following equations are used.

A.1 GAS PROPERTIES

A.1.1 Compressibility factor

Step 1: calculate pseudocritical temperature and pressure of natural gas using Sutton's correlation (Sutton, 1985), pressure, temperature and specific gravity of the gas are known at the buttomhole.

$$P_{PC} = 756.8 - 131.07\Upsilon_g - 3.6\Upsilon_g^{\,2} \quad \text{(A-1)}$$

$$T_{PC} = 169.2 + 349.5\Upsilon_g - 74\Upsilon_g^{\,2} \quad \text{(A-2)}$$

Where Υ_g is specific gravity of gas. Pressure and temperature are in psia and ^{O}R.

Step 2: calculate pseudo-reduced pressure and temperature.

$$P_{Pr} = \frac{P}{P_{PC}} \quad \text{(A-3)}$$

$$T_{Pr} = \frac{T}{T_{PC}} \quad \text{(A-4)}$$

Pressure and temperature are in psia and ^{O}R.

Step 3: The initial compressibility factor at the buttomhole depth is read from the Z-factor chart for natural gases [18]. The equation below is then used to compute for Z-factor as we go up the depth.

$$Z = \frac{2.7P\delta_g}{\rho T} \quad \text{(A-5)}$$

Step 4: calculate gas density

Gas density is determined using Lee et al (1966) correlation as shown below

$$\rho = 1.4935\, X \frac{PM}{ZT} X62.4 \qquad \text{(A-6)}$$

A.1.2 Viscosity of gas

The equation below presented by Lee et al. (1966) was used.

Step 1: calculate gas density

$$\rho = 1.4935\, X \frac{PM}{ZT} X62.4 \qquad \text{(A-7)}$$

Step2: calculate K value

$$K = \frac{(9.379+0.01607M)T^{1.5}}{(209.2+19.26M+T)} \qquad \text{(A-8)}$$

Step 3: calculate X value

$$X = 3.448 + \frac{986.4}{T} + 0.01009M \qquad \text{(A-9)}$$

Step 4: calculate Y value

$$Y = 2.447 - 0.224X \qquad \text{(A-10)}$$

$$M = 28.97\Upsilon_g \qquad \text{(A-11)}$$

Step 5: calculate gas viscosity

$$\mu_g = (10^{-4})K\exp(X\rho^Y) \qquad \text{(A-12)}$$

Gas viscosity is in centipoises, T is in ^{O}R, density is in g/cc

A.1.3 Gas formation volume factor

$$B_g = 0.0282793 \frac{ZT}{P}, \text{ft}^3/\text{Scf} \qquad \text{(A-13)}$$

Temp. is in ^{O}R and pressure is in psia.

A.1.4 Gas mass flow rate

$$\text{where } W_g = \frac{q_g \delta_g}{1130900} \quad \text{(A-14)}$$

A.2 OIL PROPERTIES

Crude oil properties are calculated with pressure, temperature, API, gas gravity known

A.2.1 Gas solubility

The gas solubility is determined from Glaso correlation (1980)

$$R_S = \delta_g \left[\left(\frac{API^{0.989}}{(T-460)^{0.172}} \right) P_b^* \right] \quad \text{(A-15)}$$

Where the correlating number $P_b^* = 10^X$ and

$$X = 2.8869 - [14.1811 - 3.3093 \log(P)]^{0.5} \quad \text{(A-16)}$$

A.2.2 Bubble point pressure of oil

Using Begg Robinson correlation

$$A = 10.715(R_S + 100)^{-0.515} \quad \text{(A-17)}$$

$$B = 5.44(R_S + 150)^{-0.33} \quad \text{(A-18)}$$

The bubble point pressure is determined by the Glaso correlation which only determines whether the oil viscosity required is saturated or undersaturated.

$$\log P_b = 1.7669 + 1.7447 \log(P_b^*) - 0.30218[\log(P_b^*)] \quad \text{(A-19)}$$

$$\text{Where } P_b^* = \left(\frac{R_S}{\delta_g} \right)^a * T^b * API^C \quad \text{(A-20)}$$

$a = 0.816, b = 0.172, C = -0.989$

A.2.3 oil formation volume factor

The following correlation was presented by Standing (1947) for pressure less than or equal to bubble point pressure.

$$B_o = 0.9759 + 0.00012F^{1.2} \quad \text{(A-21)}$$

$$\text{Where } F = R_S\left(\gamma_g/\gamma_O\right)^{0.5} + 1.25T \quad \text{(A-22)}$$

Where B_O is oil FVF in RB/STB, R_S is solution GOR in Scf/STB, T is temp in ^{O}R

A.2.4 Viscosity of oil

The dead oil viscosity is first calculated using empirical correlation by Beggs and Robinson (1975)

$$\mu_{Od} = 10^X - 1 \quad \text{(A-23)}$$

$$\text{Where } X = Y(T - 460)^{-1.63} \quad \text{(A-24)}$$

$$Y = 10^Z \quad \text{(A-25)}$$

$$Z = 3.0324 - 0.02023\,API \quad \text{(A-26)}$$

Where T is in ^{O}R

Begs and Robinson also proposed and empirical correlation for saturated oil viscosity

$$\mu_{Ob} = a(\mu_{Od})^b \quad \text{(A-27)}$$

$$\text{Where } a = 10.715(R_S + 100)^{-0.515} \quad \text{(A-28)}$$

$$b = 5.44(R_S + 150)^{-0.338} \quad \text{(A-29)}$$

Where $R_S$is the solution gas oil ratio of the liquid at P and T,μ_{Od} is the dead oil viscosity in centipoises,$\mu_{Ob}$is the oil viscosity in centipoises at at bubble point pressure.

Finally oil viscosity at reservoir condition is calculated below

$$\mu_O = \mu_{Ob}\left(\frac{P}{P_b}\right)^M \quad \text{(A-30)}$$

Where $M = 2.6P^{1.187} * 10^a$ (A-31)

$$a = -3.9(10^{-5})P - 5 \quad \text{(A-32)}$$

P is pressure above bubble point pressure, P_b is bubble point pressure in psia, μ_o isthe oil viscosity at reservoir condition.

A.2.5 Oil mass flow rate

where $W_o = \frac{(q_o \delta_o)}{246.6}$ (A-33)

A.3 Water properties

A.3.1 water formation volume factor

McCain developed a correlation for the water formation volume factor,

$$B_W = (1 + \Delta V_{wT})(1 + \Delta V_{wP}) \quad \text{(A-34)}$$

Where volume corrections for for temperature, ΔV_{wT}, and pressure, ΔV_{wP} , estimated from

$$\Delta V_{wT} = -1.00010(10^{-2}) + 1.33391(10^{-4})T + 5.50654(10^{-7})T^2 \quad \text{(A-35)}$$

$$\Delta V_{wP} = -1.95301(10^{-9})PT - 1.72834(10^{-13})P^2T - 3.58922(10^{-7})P - 2.25341(10^{-10})P^2 \quad \text{(A-36)}$$

Where B_W = water FVF, $\frac{RB}{STB}$, T = temperature, °F, and P = pressure, psia

A.3.2 Viscosity of water

Beggs and Brill correlation which considers only temperature effects was used

$$\mu_W = \exp(1.003 - 1.479(10^{-2})T + 1.982(10^{-5})T^2 \quad \text{(A-37)}$$

Where T is in °F and μ_W is in centipoises

A.3.3 Water mass flow rate

where $w_w = \frac{(q_w \delta_w)}{246.6}$ (A-38)

PRESSURE AT DEPTH

The following equation is used in extrapolating pressures in aquifers and oil and gas reservoirs

$$P_2 = P_1 \left[\exp\left(\frac{0.01877 h \Upsilon_g}{ZT}\right)\right] \quad \text{(A-39)}$$

Where h is in ft and T Is in ^{O}R

APPENDIX B

MULTIPHASE PROPERTIES

B.1 Multiphase pressure gradient equation

Begs and Brill correlation multiphase flow equation as shown below, check references for detail understanding

B.1.1 No-slip density

$$\rho_n = \rho_L \lambda_L + \rho_g \lambda_g \quad \text{for two phase} \tag{B-1}$$

$$\rho_n = \left[\rho_o \left(\frac{q_o B_o}{q_o B_o + q_w B_w}\right) + \rho_w (1 - f_o)\right] \lambda_L + \rho_g \lambda_g \quad \text{for three phase} \tag{B-2}$$

$$\text{Where } f_o = \left(\frac{q_o B_o}{q_o B_o + q_w B_w}\right) \tag{B-3}$$

$$\text{Where } \lambda_L = \lambda_o + \lambda_w = \frac{V_{so}}{V_m} + \frac{V_{sw}}{V_m}, \; f_o = \left(\frac{q_o B_o}{q_o B_o + q_w B_w}\right), \; f_w = 1 - f_o \tag{B-4}$$

$$V_{SO} = \frac{q_O}{A_P} V_{Sg} = \frac{q_g}{A_P} V_{SW} = \frac{q_w}{A_P} \tag{B-5}$$

Where the flow rate are in ft^3/sec

B.1.2 Slip or mixture density

The mixture density is obtained from

$$\rho_m = \rho_L H_L + \rho_g H_g \quad \text{for two phase} \tag{B-6}$$

$$\rho_m = \left[\rho_o \left(\frac{q_o B_o}{q_o B_o + q_w B_w}\right) + \rho_w (1 - f_o)\right] H_L + \rho_g H_g \quad \text{for three phase} \tag{B-7}$$

$$\text{Where } H_L = \frac{a \lambda_L{}^C}{N_{FR}{}^C} \text{ depending on the flow regime and } H_g = 1 - H_L \tag{B-8}$$

B.1.3 Reynolds number

Determine the liquid viscosity assuming the oil and water are mixible

$$\mu_L = \mu_O f_O + \mu_W f_W \text{for three phase} \quad \text{(B-9)}$$

$$N_{Ren} = \frac{1488\rho_n V_M d}{\mu_L \lambda_L + \mu_g \lambda_g} \quad \text{(B-10)}$$

$$f_n = {}^{1}\Big/_{[2Log\{N_{Ren}/(4.5223LogN_{Ren} - 3.8215)\}]^2} \quad \text{(B-11)}$$

B.1.4 Friction factor

$$Y = {}^{\lambda_L}\Big/_{H_L{}^2} \quad \text{(B-12)}$$

$$S = {}^{lnY}\Big/_{[-0.0523 + 3.182lnY - 0.8725(lnY^2)] + 0.01853(lnY)^4} \quad \text{(B-13)}$$

Friction factor, $f_{tP} = f_n e^S$ (B-14)

B.1.5 pressure gradient equation

$$\left(\frac{dP}{dL}\right)_{Total} = \left(\frac{dP}{dL}\right)_{Elevation} + \left(\frac{dP}{dL}\right)_{friction} + \left(\frac{dP}{dL}\right)_{accleration} \quad \text{(B-15)}$$

The pressure gradient due to acceleration from multiphase flow is usually negligible. Hence

$$\left(\frac{dP}{dL}\right)_{Total} = \frac{g}{g_c}\rho_m \sin\theta + \frac{f_{tp}\rho_n V_m{}^2}{2g_{cd}} \quad \text{(B-16)}$$

$$\tilde{\eta} = -\frac{1}{w\widetilde{C_P}}\left\{\frac{w_g}{\rho_g}\left[-\frac{T}{Z}\left(\frac{\partial Z}{\partial T}\right)_P\right] + \frac{w_L}{\rho_L}\right\} \quad \text{(B-17)}$$

From Sutton's correlation for z factor

$$Z = \frac{2.7P\delta_g}{\rho T} \quad \text{(B-18)}$$

$$\rho = \frac{2.7P\delta_g}{ZT} \quad \text{(B-19)}$$

$$\left(\frac{\partial Z}{\partial T}\right)_P = -\frac{2.7P\delta_g}{\rho T^2} \quad \text{(B-20)}$$

Substituting the differential of Z-factor with respect to temperature at constant pressure, and also the equation for the density of gas into the average Joule Thompson coefficient, it becomes

$$\tilde{\eta} = -\frac{1}{w\widetilde{C_P}}\left\{\frac{w_g}{\rho_g} + \frac{w_L}{\rho_L}\right\} \quad \text{(B-21)}$$

The above equation is substituted into the dimensionless parameter

$$\Phi = \left[\rho\eta C_P \frac{dP}{dL} - \rho g \sin\theta - \rho v \frac{dv}{dL}\right] / \frac{dP}{dL} \quad \text{(B-22)}$$

$$T = (T_{ei} - g_e L \sin\theta) + (T_i - T_{ei})e^{\frac{-L}{A}} + g_e A \sin\theta\left(1 - e^{\frac{-L}{A}}\right) + \frac{1}{\rho C_P}\Phi A \frac{dP}{dL}\left(1 - e^{\frac{-L}{A}}\right) \quad \text{(B-23)}$$

APPENDIX C

WELLBORE PROFILE

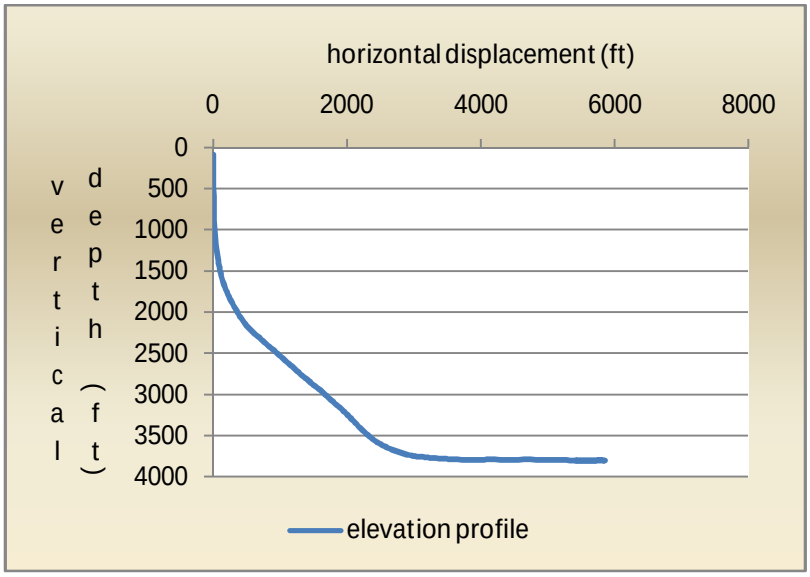

Figure A1. Wellbore profile of vertical depth versus horizontal displacement

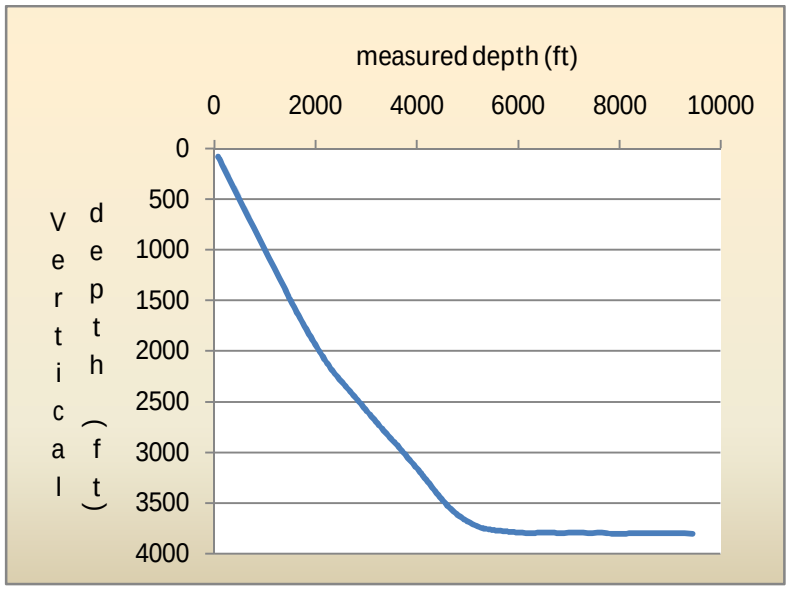

Figure A2. Wellbore profile of vertical depth versus measured depth

Gauge measure depth = 4543.11 ft

Gauge vertical depth =3491.41